Classified Index: TK715
U.D.C: 621.3

Dissertation for the Academic Master's Degree

Research of game-theoretic scheduling in integrated energy system considering energy flexibility from consumers

Candidate: LiXin

Supervisor: Prof. Yang Guotian

Academic Degree Applied for: Master of Engineering

Subject: Control Science and Engineering

Speciality: Pattern recognition and intelligent system

School: School of Control and Computer Engineer

Date of Defence: May, 2022

Degree-Conferring-Institution: North China Electric Power University

Abstract

In regard to scheduling of integrated energy systems, apart from optimising the integrated energy system itself, how to exploit the flexibility from the customers' side while taking into account the customer's satisfaction is a problem that needs to be solved. In this paper, I propose a master-slave game based on integrated energy flexible load scheduling method.

The paper first establishes an energy satisfaction and utility model based on the consumer's experience of using energy. Compared to questionnaires, unreliable functional expressions or vague prediction and evaluation voting models, the satisfaction and utility model provides a clear picture of the benefits of consumers' energy use experience. The utility function proposed in this paper also takes into account the effect of the amount paid by the customer on the satisfaction of energy use, thus more closely matching the actual customer experience. At the same time, this paper designs a comprehensive energy system model that includes a cooling, heating and power triple-supply system, a heat pump system, a distributed power generation system and an energy storage system, and establishes its operational objectives and operational constraints. On this basis, the paper further proposes a flexible load dispatching method based on a hierarchical master-slave game, in which the energy benefits saved in the actual flexible load dispatching method are reasonably allocated through a hierarchical game of one master and multiple slaves to achieve a balanced optimisation of the customer's energy consumption experience and the operation of the integrated energy system. In order to solve the proposed game model, this paper introduces and uses the GBO (Graph Based Optimization) algorithm to implement a dynamic game equilibrium solution to obtain the game solution results at each point in time. Then, the paper presents a validation of the algorithm for different seasonal scenarios. The results of the integrated energy system and the energy utility functions of the consumers are analysed for different seasonal temperature conditions in the scenarios. The analysis of the economic indicators of the example shows a significant reduction in both system costs and consumer fees, specifically, 20.65% and 20.21% in winter, 15.97% and 13.32% in spring and autumn, and 11.42% and 8.25% in summer. The results show that the game based flexible load scheduling for integrated energy consumers can save energy costs for both the integrated energy system and the consumers, and validate the effectiveness of the scheduling method proposed in this paper.

Keywords: Integrated Energy System, Consumers, Flexible Scheduling, game-

theoretic

Content

1 Introduction

1.1 Background

In the face of the severe environmental challenges and energy shortages caused by the large-scale consumption of fossil fuels, the world's energy situation is encountering significant hurdles. There is a growing focus on renewable energy as people increasingly recognize the need for its development in order to achieve a sustainable future. This transition towards renewable and sustainable energy sources has become a global consensus[1].To address this global issue, extensive efforts are currently underway to construct smart grids, aiming to facilitate the greater utilization of renewable energy generation[2]. However, due to the limited adaptability of smart grids, the issue of renewable energy curtailment remains a significant challenge within existing energy systems. "The Third Industrial Revolution", a book[3], proposes that by integrating various forms of energy and establishing grid-centered intelligent integrated energy systems, the traditional patterns of energy consumption can be transformed, thereby stimulating the growth of renewable energy.

With the development of digital high-tech technologies, represented by big data, artificial intelligence, and advanced communication technologies, the integration of these technologies with traditional power and energy systems has become a crucial support for the comprehensive development of China's future energy industry. China has also formulated supportive policies and development plans to promote the progress of integrated energy[4]. Simultaneously, many countries worldwide have implemented policies and plans to accelerate the development of integrated energy. For instance, the European Union's "Horizon 2020" program and the United Kingdom's "Energy System Catapult" initiative are notable examples.

In recent years, with the expansion of microgrid structures and the rapid development of multi-energy systems and energy internet, various forms of energy coupling in the fields of energy production, transmission, and consumption have become increasingly interconnected. This has led to the emergence of Integrated Energy Systems (IES) as a new energy system structure. Integrated Energy Systems combine various distributed energy sources with traditional energy sources (such as electricity, gas, heat, and cold), creating an effective way of cascading and utilizing energy efficiently. IES[5] is a system that couples different energy sources, such as cooling, heating, and electricity, while coordinating the integration of multiple energy sources, loads, and energy

storage in a vertical source-grid-load-storage manner. It significantly enhances energy utilization efficiency, improves the integration of renewable energy, reduces system operation costs, and lowers emissions of pollutants like carbon dioxide[6].

The urgent need for energy transition currently places higher demands on the rapid implementation of Integrated Energy Systems (IES). Therefore, in-depth research is necessary to bridge the gap between theoretical advancements and practical applications of IES, with a particular focus on key technologies. Among these technologies, the most crucial one is the optimization of IES dispatch. A central topic in current research on Integrated Energy Systems is the exploration of methods to enhance the capabilities of dispatch optimization. Investigating how to improve the scheduling and optimization of Integrated Energy Systems is paramount to the advancement of IES research.

1.2 Literarue reviwe

1.2.1 IES operating

Integrated Energy Systems (IES) can integrate multiple energy systems, such as power supply, heating, cooling, and energy storage, allowing for efficient fulfilment of various energy demands. The integration of diverse systems, including heating, power, cooling, renewable energy, and energy storage, within an IES greatly enhances the overall environmental, economic, and technological benefits[8]. A Combined Cooling, Heating, and Power (CCHP) system provides an effective solution for integrating multiple energy sectors, as it can simultaneously meet the requirements for heating, electricity, and cooling[9]. Furthermore, since the CCHP system generates power locally, it functions as a distributed energy system, effectively reducing the peak load on the grid[10]. Numerous studies have shown that implementing CCHP systems in residential buildings[11], commercial buildings[12], and industrial sectors[13] can achieve high energy efficiency and yield significant environmental and economic benefits.

The power generation unit (PGU) in a CCHP system utilizes fuel combustion, typically natural gas, to generate electricity. The related waste heat is recovered for space heating through a heat recovery boiler or used by absorption chillers to meet cooling demands[14]. Typically, CCHP systems operate based on either Following the Thermal Load (FTL) or Following the Electricity Loads (FEL) strategies[15]. Due to the mismatch between heat and electricity demands, there may be short periods of energy shortage or surplus. Therefore, the integration of various technologies with CCHP systems is necessary to address these energy imbalances and further enhance the

overall system efficiency. These technologies include waste heat recovery systems, lithium bromide absorption chillers, heat pump systems, photovoltaic (PV) generators, wind power systems, energy storage systems, and thermal storage systems[16]. In addition to equipment-level technologies, the system can benefit from purchasing electricity from the grid to improve the performance of CCHP systems[17]. The combination of these technologies has been successful. However, the focus of these studies lies in the system's construction, and there is potential for further improvements, particularly in terms of overall operation and load distribution optimization at a larger scale.

In an Integrated Energy System (IES), various energy devices are closely coupled and capable of flexible conversion, making it a complex task to determine the optimal energy management and operational strategies. In this regard, significant progress has been made in current research. Reference[18] introduces the concept of an Energy Hub (EH), laying the theoretical foundation for subsequent optimization studies of IES. Building upon this concept, reference[19] proposes a graph-theory-based modelling approach using an Integrated Energy Standardization Matrix, which aids in the practical application of IES planning and operation. Reference[19] also introduces and models cogeneration technologies, gas-fired power plants, pumped storage systems, gas storage facilities, thermal buffer tanks, wind turbines, as well as the role of electricity and gas network constraints. Reference[20] presents an operational methodology for a multi-carrier energy system, ensuring the energy network functions to meet daily electricity, gas, heating, and water demand. Reference[21] proposes an optimal operation approach for IES considering the involvement of electricity, gas, and heat distribution networks.

However, the output of various types of integrated energy devices and loads exhibits stochastic and volatile characteristics, introducing uncertainties into energy scheduling for IES. To address such issues[22], scholars have proposed using robust optimization, stochastic optimization, or fuzzy optimization to account for uncertainty factors[23]. Reference[24] addresses thermal energy storage technology and presents a robust operation model to coordinate multi-carrier systems, including electricity, gas, heat, and water carriers, enabling the scheduling system to make appropriate decisions in response to potential changes in power load. Additionally, reference[24] considers the volatility of wind power, load electricity, and energy prices, proposing a stochastic optimization approach that accounts for multiple uncertainties. To address the differences in response times for electricity, gas, heat, and cooling, reference[25] presents an optimization approach for IES considering multiple time scales. Building

upon this, a mixed time-scale operational optimization framework for IES is established[26], achieving dynamic coordinated optimization of multi-energy systems involving electricity, gas, and heat. Furthermore, with increasing participation of social capital in energy market transactions, the operational planning and energy market domains of IES exhibit diversified characteristics[27]. Reference[28] proposes a day-ahead scheduling strategy for IES in an energy service market environment, effectively combining diverse energy demands from different regions. Based on this, reference [29] establishes a two-level transactional energy trading framework, which enhances the energy scheduling and operational efficiency of multi-carrier energy systems effectively.

The previous analysis discussed the system architecture and optimization strategies of an Integrated Energy System (IES), with a focus on operational optimization and scheduling methods. However, optimizing the equipment and operational scheduling of the IES alone is not sufficient. It is equally important to optimize from the source. As the coupling of multiple energy types deepens within the IES, the role of demand-side becomes increasingly significant in system operation. Reference[30] introduces the concept and framework of Integrated Demand Response (IDR), which provides guidance for involving energy consumers in system optimization and regulation. In reference[31], IDR is integrated into energy management from the perspectives of energy transfer and environmental-economic dispatch, and the effects of IDR methods are further studied and analyzed. Building upon the theory of demand response, flexible load scheduling of the IES[32] has recently emerged as a research hotspot.

1.2.2 Demand flexibility

The continuously changing load demand has always been a major source of uncertainty in energy systems[33]. In an Integrated Energy System (IES), the integration complexity introduces randomness and volatility, posing challenges of increased uncertainty and reduced controllability in system scheduling. With a high share of renewable energy sources in the IES, there are issues of control instability in actual dispatch operations. To address this problem, new methods need to be designed to control generation or demand. On the generation side, although the uncertainty of renewable energy can be controlled to some extent through scheduling[34], the power output cannot be increased due to fixed wind and radiation conditions. In contrast, exploring ways to improve controllability on the demand side is also a crucial direction [35]. Besides relying on the establishment of energy storage systems to enhance the controllability of the IES, flexible control of conventional demand can be utilized for flexibility-based scheduling[36].

Flexible control of demand for flexibility-based scheduling can achieve effects similar to increasing supply. Generally, while it is relatively easy to predict how much power a generation unit can provide[37], accurately obtaining energy demand with a certain degree of flexibility is not straightforward. As discussed in reference[38], the flexibility of flexibility-based scheduling for home heating depends on its usage pattern. For example, when the user is at home, the allowable temperature variation may be smaller compared to when the user is at work. This means that the flexibility range of flexibility-based scheduling depends not only on assessing the available flexibility but also on evaluating the user's energy usage status. As described in reference [38], flexible scheduling ultimately needs to be aligned with user preferences, and the flexibility-based scheduling of the IES can only proceed if it meets the user's energy demands. However, as mentioned in reference[39], most energy systems' flexibility-based scheduling can only be achieved through indirect control based on prices[40]. In such cases, grid operators send different prices to the IES with flexibility-based scheduling based on certain contractual agreements[41], rather than directly controlling energy flexibility. While there is still an expectation of improving the flexibility of energy systems through price control, the ultimate decision lies with the system owner. This approach often encounters challenges in practice, such as dealing with situations where users are unwilling to participate in flexible scheduling or the uncertainty in people's responses to price changes[42].

Therefore, while flexibility-based scheduling can be achieved through certain demand control measures or indirect price controls, the former may struggle to guarantee a satisfactory user energy experience, and the latter may fail to ensure desired user control outcomes. Therefore, there is a need for a flexibility-based scheduling approach that can simultaneously ensure a satisfactory user energy experience and achieve significant load reduction.

The user's energy experience and satisfaction are primarily determined by three factors[43]: thermal comfort, visual comfort, and appliance usage satisfaction. Thermal comfort is mainly met through heating and cooling systems, while the power supply system caters to the user's electricity demands for visual comfort and appliance usage satisfaction. Currently, there are two main methods for estimating user energy preferences and satisfaction. The first method involves conducting questionnaire surveys after designing a comprehensive evaluation system. For example, Lizhen Wang[44] proposed a quantitative study based on Energy-Environment-Satisfaction (EES) to analyze the distribution characteristics of EES parameters in a three-star green

building in Shanghai. The author designed a user satisfaction evaluation system based on indoor environmental parameters and conducted a questionnaire survey. By collecting 43 questionnaires, an estimation of user satisfaction was obtained. However, questionnaire surveys may not capture energy satisfaction in most cases, and they are limited in representing user energy satisfaction across all time periods. The second method involves expressing user satisfaction through utility functions. In [45,46], the authors used quadratic functions to express consumer satisfaction and incorporated them into the overall utility function. In fact, in the study presented in[47], users' satisfaction with different energy consumption needs was found to vary, but the specific satisfaction functions were not provided. Therefore, using utility functions may not guarantee the reliability of the function itself and the coefficients used.

What has been largely overlooked by most researchers is the established measurement indicator for thermal comfort in the HVAC field, known as the Predicted Mean Vote (PMV) proposed by Fanger[48]. The PMV extends the comfort equation to a seven-point scale of the ASHRAE (American Society of Heating, Refrigerating and Air-Conditioning Engineers) thermal sensation scale (-3 cold, -2 cool, -1 slightly cool, 0 neutral, +1 slightly warm, +2 warm, +3 hot). This indicator is widely used to assess thermal comfort provided by heating and cooling systems. While the seven-point scale of the Predicted Mean Vote aligns closely with human perception, it is difficult to convert into numerical values representing actual satisfaction. Therefore, the Predicted Percentage of Dissatisfied (PPD) has been extensively used[49] to measure and calculate actual thermal comfort satisfaction. Additionally, for electricity usage assessment, researchers such as Sally et al. [50] pointed out that each electrical device in the actual electricity consumption process provides users with different levels of comfort and satisfaction. Hence, the satisfaction of electricity usage can be calculated based on the expectation of total electricity usage and the actual amount of electricity supplied. Furthermore, in Ref.[51], the ratio of satisfaction to charges was proposed to accurately measure the user's energy experience.

Moreover, it is observed that there is a conflict between maximizing the user's energy experience and maximizing the benefits of flexibility-based scheduling in a comprehensive energy system. Once flexibility-based scheduling is implemented on the demand side, the user's energy experience will inevitably be affected. Achieving a balance between enhancing the user's energy experience and improving the benefits of flexibility-based scheduling in the comprehensive energy system requires an approach based on game theory to achieve a reasonable equilibrium for both parties.

1.2.3 Game theory in IES

In the field of energy dispatch and energy trading operations in integrated energy systems, game theory methods are widely used. Typically, after the model is developed, game theory is employed to determine the Nash equilibrium (NE), which maximizes the profit for all participants. In this equilibrium, no player has the incentive to change their strategy because they cannot gain more benefits by deviating from it[52]. In Ref. [53], a Bayesian game model was used to formulate the scheduling of electric vehicle energy consumption in bidirectional energy trading. Their optimal solution was obtained through Bayesian Nash equilibrium. Besides these models, the Cournot model with duopoly and oligopoly models is extensively used. In Ref. [54], the Cournot oligopoly model was employed for a three-player competition in a transmission-constrained system considering non-constant marginal costs to derive the equilibrium point. In Ref.[55], the profit-maximizing behavior of agents in wholesale markets was formulated and solved. In Ref. [56], the Cournot oligopoly model was used to analyze nodal prices and transmission constraints in multiple markets. In Ref. [57], considering energy arbitrage and imperfect competition among suppliers, the Cournot oligopoly model was utilized for solution.

Furthermore, considering that in energy trading schemes, some participants may have the priority to decide their strategies over others, particularly in the case of Stackelberg games. The Stackelberg game is a non-cooperative game theory approach that clearly distinguishes participants into leaders and followers based on their sequential actions. Several interesting leader-follower models have been developed to analyze interactions between energy suppliers and consumers, categorizing them into single-leader multiple-followers (SLMF) models and multiple-leader multiple-followers (MLMF) models. In the context of SLMF games, [58] and [59] solved energy management problems by simulating electricity users and multiple electricity sectors as leaders and followers, respectively. Conversely, [60] assigned the role of the leader in the game to the utility company interacting with electricity users based on prices. Regarding MLMF games[61], Ref. [62] proposed an energy trading mechanism for multiple microgrids that considered price competition among electricity buyers, who act as followers in the game. [63] presented a demand response management mechanism in smart grids where multiple utility companies serve as leaders, representing followers. However, all the aforementioned studies mainly focused on electricity trading. Recent research[64] employed static game methods to investigate energy trading problems considering multiple energy sources, but they only considered the quantity of energy traded, treating energy prices as output functions. Moreover, these studies overlooked

the benefits of user engagement in future energy markets[65].

Among the aforementioned research, few studies have concentrated on using a hierarchical dynamic single-leader multiple-followers (SLMF) model. The dynamic variations in the multi-energy supply-demand relationship between integrated energy systems and users during actual dispatch lead to different game outcomes in each iteration. Additionally, due to the complexity introduced by multiple followers, the hierarchical approach can significantly enhance the speed and accuracy of game solution.

1.3 Main Framework

The current state of integrated energy scheduling is reviewed in the comprehensive literature. This paper proposes a comprehensive energy dispatch method based on master-slave game theory to address the flexibility scheduling problem in integrated energy systems. To capture the user energy experience and satisfaction, a utility model based on user energy experience is established. This utility model provides a clear representation of the user's energy experience benefits, taking into account the influence of user payment limits on energy satisfaction. Compared to impractical questionnaire surveys, unreliable function expression methods, or fuzzy PWM prediction evaluation voting models, the utility model effectively characterizes the user's energy experience benefits while considering the impact of user payment limits on energy satisfaction. Based on the utility model and the established integrated energy system operation model, this paper further proposes a master-slave game-based flexible load scheduling method. By employing a hierarchical game with one master and multiple slaves, the method allocates the energy benefits saved in the actual flexible load scheduling optimally, achieving a balance between user energy experience and the operation of the integrated energy system. The dynamic game equilibrium is achieved through the GBO (Game-Based Optimization) algorithm, obtaining the game solution results at different time points. Furthermore, case studies are conducted considering different seasonal scenarios. The effectiveness of the proposed scheduling method is validated through economic dispatch analysis and sensitivity analysis regarding variations in user energy metabolism rates.

The main research work and structure of the paper are roughly as follows:
Chapter 1: Introduction
In this chapter, the background of integrated energy systems is discussed in Section 1.1, highlighting the significance of the research in addressing current issues. Section

1.2 provides an overview of the research status in integrated energy system scheduling, flexibility scheduling, user energy experience, and the application of game theory in integrated energy scheduling. Finally, Section 1.3 outlines the main research work and structure of the article.

Chapter 2: User Energy Model and System Operation Model of Integrated Energy
This chapter begins with an analysis of user energy satisfaction in Section 2.1, where evaluation models for user thermal and cold satisfaction and electricity usage satisfaction are established. Based on these models, a comprehensive user energy utility model is constructed to describe the combined benefits of user comfort and cost in energy consumption. Section 2.2 focuses on modeling the main components of the integrated energy system, including the system operator, equipment, operation objectives, and constraints, to establish the system operation model. Finally, Section 2.3 provides a summary of the chapter.

Chapter 3: Master-Slave Game-Based Flexible Load Scheduling Method
This chapter introduces the flexible load scheduling model in Section 3.1, combining the user energy model from Section 2.1 and the system operation model from Section 2.2 to improve user energy benefits in the scheduling process. Section 3.2 introduces the concept of master-slave game theory and establishes a hierarchical master-slave game-based flexible load scheduling model. The existence theorem for equilibrium solutions in the master-slave game is presented, demonstrating the existence of equilibrium solutions for the proposed model. In Section 3.3, the GBO algorithm is introduced, along with the solution process for the master-slave game-based flexible load scheduling model using the GBO algorithm. Finally, Section 3.4 summarizes the content of Chapter 3.

Chapter 4: Case Analysis
This chapter provides the configuration data for simulation in Section 4.1, including system equipment capacities, rated power, and relevant economic parameters, as well as user states, seasonal scenarios, and distributed generation system output predictions. Section 4.2 analyzes the scheduling results for different seasonal scenarios, including the output and supply status of the integrated energy system equipment, indoor temperature, thermal satisfaction, and electricity satisfaction of users. Economic analysis of the results is also conducted. Lastly, in Section 4.3, sensitivity analysis is performed to examine the influence of energy metabolism rates and user state variations on the scheduling results.
Chapter 5: Conclusion and Future Work

This chapter provides a brief summary of the entire paper, highlighting the research achievements. It also discusses the limitations of the proposed integrated energy user flexible load scheduling method and suggests directions for future research.

2 Consumer modelling and IES modelling

2.1Consumer Modelling

In the practical operation and scheduling of integrated energy systems, the primary objective is to meet the users' energy demands while maximizing the cost-effectiveness of the overall system. Therefore, it is necessary to first model the energy demands and satisfaction of integrated energy system users. Subsequently, when modelling the operation of the integrated energy system, constraints should be included to ensure the satisfaction of user energy demands.

2.1.1 Consumer comfort modelling

In the context of user experience, thermal comfort plays a significant role in overall user satisfaction with energy consumption. However, measuring thermal comfort can be complex due to the subjective nature of human thermal perception. Heating and cooling are crucial components of energy consumption, and it is important to quantitatively measure thermal comfort to assess the effectiveness of heating and cooling systems.

Currently, the primary evaluation indicators for thermal comfort are the Predicted Mean Vote (PMV) and the Predicted Percentage of Dissatisfied (PPD). PMV extends the comfort equation to a seven-point thermal sensation scale defined by the American Society of Heating, Refrigerating, and Air-Conditioning Engineers (ASHRAE). The scale ranges from -3 (cold) to +3 (hot). The PMV equation, as defined by Fanger [66] , is quite complex and can be expressed as follows:

$$PMV = (0.303e^{-0.036M} + 0.028) \cdot [(M - W) - E_s - E_b - C_b - H] \quad (2\text{-}1)$$

Where PMV —— The Predicted Mean Vote；

M —— The consumers' energy metabolism rate， W / m^2；

W —— The mechanical work performed by the human body, which is typically negligible or close to zero, W / m^2；

E_s —— The heat carried away by the evaporation of sweat on the skin；

E_b —— The heat carried away by evaporation during the breathing process；

C_b —— The heat generated by convection during the breathing process；

H —— Sensible heat loses from radiation and convection；

The heat loss due to sweat evaporation E_s can be calculated using the following equation.

$$E_s = -3.05 \cdot 10^{-3} \cdot [5773 - 6.99 \cdot (M - W) - p_a] \quad (2\text{-}2)$$

Where p_a ——vapour pressure of water in the surrounding indoor environment；

The heat dissipated through evaporation during respiration E_b can be expressed as:

$$E_b = 1.7 \cdot 10^{-5} M \cdot (5876 - p_a) \quad (2\text{-}3)$$

The heat generated by convection during the process of respiration can be calculated using the following equation.

$$C_b = 0.0014M \cdot (34 - t_a) \quad (2\text{-}4)$$

Where t_a ——temperature of the indoor environment；

The sensitive heat loss from radiation and convection from the skin H can be represented as:

$$H = 3.96 \cdot 10^{-8} \cdot f_{cl} \cdot [(t_{cl} + 273)^4 - (t_r + 273)^4] - f_{cl} h_c (t_{cl} - t_a) \quad (2\text{-}5)$$

Where t_a —— temperature of the indoor environment；

t_{cl} —— surface temperature of the clothing；

h_c —— convective heat transfer coefficient；

t_r —— average radiation temperature；

f_{cl} —— clothing area factor (the ratio of the clothed surface area to the naked surface area)；

According to the study in reference [67], it can be simplified in practice as a function of the indoor temperature within a certain temperature range.

$$PMV_{i,t} = a_1 \cdot T_{i,t}^{in} + b_1, t \in [T^c, T^d] \quad (2\text{-}6)$$

Where $PMV_{i,t}$ —— predicted mean vote of the consumer group i at time t；

M —— energy metabolism rate of the user group, measured in W / m^2；

a_1、b_1—— constants in Equation(2-6)；

$T_{i,t}^{in}$ —— indoor temperature of the consumer group i at time t；

T^c、T^d —— upper and lower limits of the indoor temperature；

The indoor temperature is primarily influenced by the external temperature and the

heating or cooling provided by the integrated energy system. The specific calculation expression[67] is given as follows:

$$T_{i,t+1}^{in} = T_{i,t}^{in} - \frac{\Delta T}{C \cdot R} \cdot [T_{i,t}^{in} - T_{i,t}^{out} - \frac{1.75}{Q^{\max}} u_{i,Q}(t) \cdot R \cdot Q_{i,t} + \frac{1.75}{H^{\max}} u_{i,H}(t) \cdot R \cdot H_{i,t}] \quad (2\text{-}7)$$

Where $T_{i,t}^{in}$ 、 $T_{i,t}^{out}$ —— indoor and outdoor temperatures of the consumer group i at time t;

C、R—— capacity and thermal resistance of the heating or cooling system;

$u_{i,Q}(t)$、$u_{i,H}(t)$—— indicator variable that represents whether heating or cooling is active at time t (1 for active, 0 otherwise);

$Q_{i,t}$、$H_{i,t}$—— the cooling and heating load;

$Q^{\max}$、$H^{\max}$——maximum value between the cooling and heating loads;

$$PPD(PMV_{i,t})_{i,t} = 100 - 95 \times \exp[-(0.003353 \times PMV_{i,t}^4 + 0.2179 \times PMV_{i,t}^2)] \quad (2\text{-}8)$$

Where $PPD_{i,t}$ ——predicted percentage of dissatisfaction of the consumer group i at time t;

$$PTS_{i,t} = 1 - PPD_{i,t} / 100 \quad (2\text{-}9)$$

Where $PTS_{i,t}$ —— thermal satisfaction percentage of the consumer group i at time t;

In addition to the requirements for thermal comfort, another important goal of energy consumer is electricity consumption satisfaction, which is mainly determined by the extent to which their expectations for using electrical appliances are met. It is represented as the percentage of obtained electricity to the desired electricity consumption. The specific expression is as follows:

$$PES_{i,t} = P_{i,t}^{E} / E_{i,t} \quad (2\text{-}10)$$

Where $PES_{i,t}$ —— Percentage of electricity consumption satisfaction for the consumer group i at time t;

$P_{i,t}^{E}$ —— Total power supplied to the consumer group i for electricity at time t;

$E_{i,t}$ —— Total power demanded by the consumer group i for electricity at time t;

According to equations (2-1)-(2-9), we have established the relationships between indoor temperature variations and user satisfaction. Due to the relative ambiguity of the PMV index, the PPD is often used as a practical descriptive index [49]. However, according to the study by Ogunjuyigbe[51], satisfaction is more conveniently incorporated into a function considering satisfaction and economic costs. Therefore, we use PTS as a substitute for PPD as a mathematical indicator to describe user satisfaction.

However, equations (2-8) and (2-9) show that the relationship between PTS and PMV is complex and nonlinear. If we were to incorporate it into a typical mixed-integer programming model, the computational process would become complicated. To address this issue, we employ a piecewise linearization algorithm to linearize and simplify the relationship.

First, we set $b_1 \le b_2 \le \ldots \le b_n \le b_{n+1}$ as the division point for the piecewise linear function and define:

$$b_1 = PMV_{\min}, b_k = PMV_{\min} + k \cdot \frac{PMV_{\max} - PMV_{\min}}{n}, b_{n+1} = PMV_{\max}, k = 2,\ldots,n \quad (2\text{-}11)$$

Where—— $PMV_{\min}$ and $PMV_{\max}$ are the minimum and maximum value of the predicted mean vote corresponding to the acceptable lowest and highest indoor temperatures, respectively.

By introducing auxiliary variables $\gamma_{i,t,k}, k = 1\ldots n+1$, as well as the piecewise linear function $PTS_{i,t}^{linear}$, the non-linear function (2-8) can be transformed into a mixed-integer programming model, yielding the following result:

$$PTS_{i,t}^{linear} = \sum_{k=1}^{n+1} [PTS(b_k)_{i,t} \cdot \gamma_{i,t,k}] \quad (2\text{-}12)$$

$$PMV_{i,t} = \sum_{k=1}^{n+1} b_k \cdot \gamma_{i,t,k} \quad (2\text{-}13)$$

$$s.t. \begin{cases} \gamma_{i,t,1} \le \kappa_{i,t,1}, \gamma_{i,t,n+1} \le \kappa_{i,t,n+1}, \gamma_{i,t,k} \le \sum_{j=k-1}^{k} \kappa_{i,t,j}, k = 2\ldots n \\ \sum_{k=1}^{n} \gamma_{i,t,k} = 1 \\ \sum_{k=1}^{n} \kappa_{i,t,k} = 1 \end{cases} \quad (2\text{-}14)$$

2.1.2 Consumer incentive and objective

Integrated energy systems provide consumers with varying levels of comfort and satisfaction during a day through the provision of heating, cooling, and electricity. However, as integrated energy systems have their own costs and profit requirements, consumers are charged for the services provided. In most cases, the operators of integrated energy systems bill consumers based on their energy consumption. Most research focuses on determining the optimal energy supply methods, sizes, and timing that maximize consumer satisfaction. In this regard, Ogunjuyigbe et al. [51] further developed a unit cost satisfaction index that relates consumer expenditure to achieved satisfaction. The unit satisfaction cost represents the amount of money required for a unit of satisfaction obtained by the consumer. According to Ogunjuyigbe et al. [51], this index provides a more accurate representation of the consumers' actual energy experience. The specific expression is as follows:

$$SA_{i,t} = \frac{PES_{i,t}}{CE_{i,t}} \cdot \frac{PTS_{i,t}}{CT_{i,t}} \tag{2-15}$$

Where $SA_{i,t}$ —— The unit energy satisfaction percentage of the consumer group i at time t;

$CE_{i,t}$ —— The electricity cost of the consumer group i at time;

$CT_{i,t}$ —— The heating and cooling cost of the consumer group i at time;

In practical dispatching, it is crucial to balance the economic efficiency of the integrated energy system dispatch with the actual user experience, as users play the dual role of energy consumers and payers. This objective needs to be given significant consideration when scheduling the integrated energy system.

2.2IES modelling

An integrated energy system is a complex multi-input multi-output energy system, where various energy devices are interconnected and interact with each other. To analyse the operation and optimise the scheduling process, it is necessary to first model the equipment and dispatching outputs of the integrated energy system.

2.2.1 Main system

The structure of an integrated energy system mainly consists of external energy inputs, distributed units, energy management systems, energy coordination devices, and loads. It optimally schedules multiple energy devices to generate and distribute energy in the

form of cooling, heating, electricity, etc., to meet the energy demands of users with multi-scale uncertainties, thereby achieving economically and sustainably energy supply.

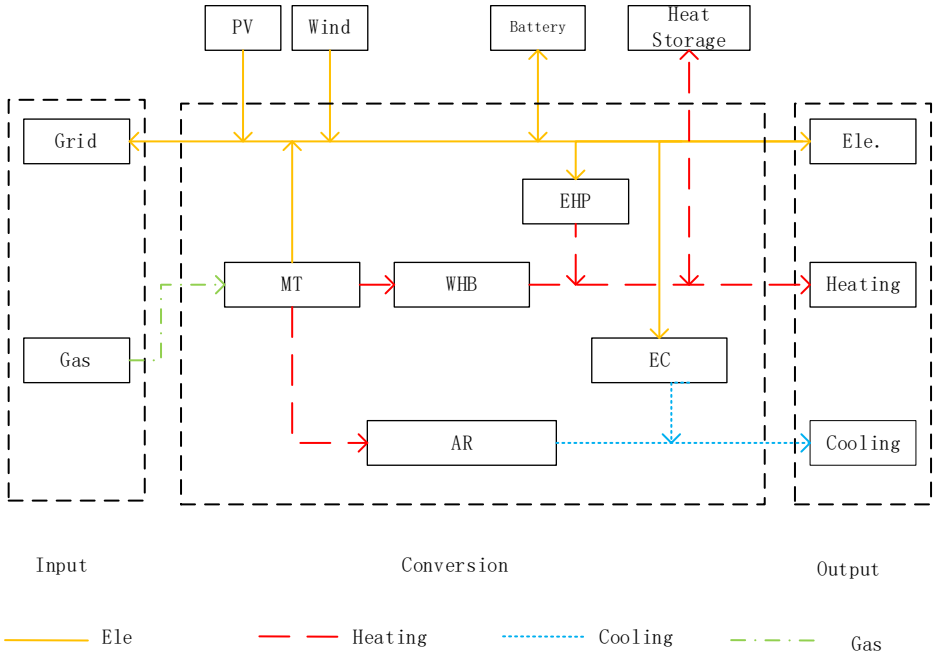

Figure 2-1 Integrated Energy System Structure Diagram

The structure of the integrated energy system is illustrated in Figure 2-1. The system primarily consists of a Combined Cooling, Heating, and Power (CCHP) system, a heat pump system, a distributed power generation system, and an energy storage system, enabling the scheduling of electricity, heat, and cooling energy.

The electrical energy in the system is mainly supplied by the gas turbines in the distributed power generation system and the CCHP system, which meets the electricity demand and powers the heat pump system. The electrical network incorporates a battery storage system that charges during surplus electricity and discharges during electricity shortage, serving the purpose of peak shaving and load shifting. Additionally, the system is interconnected with the main power grid, allowing for electricity purchase from the grid during low market prices or high electrical demand.

The heat energy is sourced from the waste heat boilers and the heat pump system in the CCHP system, primarily catering to the heat load demands of users. The heat network integrates a thermal storage tank system that absorbs heat when there is sufficient heat supply and releases heat when there is a shortage. The cooling load is primarily supplied by the heat pump system and the absorption chillers in the CCHP system.

2.2.2 Device model

The Combined Cooling, Heating, and Power (CCHP) system consists of several key components, including a gas turbine, waste heat boiler, and absorption chiller.

The model for a micro gas turbine is defined as follows:

$$P_{i,s,t}^{\mathrm{MT}} = \frac{\eta_{i,s,t}^{\mathrm{MT}} C_{i,s,t}^{\mathrm{MT}}}{R_{\mathrm{gas}}} \cdot LH \tag{2-16}$$

Where $P_{i,s,t}^{\mathrm{MT}}$ —— Output power of the micro turbine i in scenario s at time t;

$\eta_{i,s,t}^{\mathrm{MT}}$ —— Generation efficiency of the micro turbine i in scenario s at time t;

$C_{i,s,t}^{\mathrm{MT}}$ —— Fuel cost of the micro turbine i in scenario s at time t;

R_{gas}、LH —— Gas price and average calorific value of gas;

$$P_{\min}^{\mathrm{MT}} \le P_{i,s,t}^{\mathrm{MT}} \le P_{\max}^{\mathrm{MT}} \tag{2-17}$$

Where $P_{\min}^{\mathrm{MT}}$ —— Minimum output power of the micro turbine;

$P_{\max}^{\mathrm{MT}}$ —— Maximum output power of the micro turbine;

Due to the inertia of the micro turbine during operation, it is difficult to make significant power changes within a short period. Therefore, there are upper and lower limits on the power variation for the micro turbine:

$$\Delta P_{\min}^{\mathrm{MT}} \le P_{i,s,t_0}^{\mathrm{MT}} - P_{i,s,t_0-\Delta t}^{\mathrm{MT}} \le \Delta P_{\max}^{\mathrm{MT}} \tag{2-18}$$

Where $P_{i,s,t_0}^{\mathrm{MT}}$ —— Output power of the micro turbine i in scenario s at time t_0;

$P_{i,s,t_0-\Delta t}^{\mathrm{MT}}$ —— Output power of the micro turbine i in scenario s at time $t_0-\Delta t$;

$\Delta P_{\min}^{\mathrm{MT}}$ —— Minimum fluctuation power of the micro turbine;

$\Delta P_{\max}^{\mathrm{MT}}$ —— Maximum fluctuation power of the micro turbine;

The mathematical model of the absorption refrigeration system is as follows:

$$Q_{i,s,t}^{\mathrm{AR}} = \frac{P_{\mathrm{MT}}(t)}{\eta_{i,s,t}^{\mathrm{MT}}} \cdot \xi_{i,s,t}^{\mathrm{AR}} (1-\eta_{i,s,t}^{\mathrm{MT}} - \eta_l) \cdot COP_{i,s,t}^{\mathrm{AR}} \tag{2-19}$$

Where $Q_{i,s,t}^{\mathrm{AR}}$ —— cooling capacity of absorption refrigeration i in the scene s at the time t;

$\xi_{i,s,t}^{\mathrm{AR}}$ ——proportion of waste heat obtained by the absorption refrigeration i in the scene s at the time t relative to the total waste heat from the micro turbine;

η_l —— loss of waste heat during the transmission process of the micro turbine;

$COP_{i,s,t}^{\mathrm{AR}}$ —— cooling efficiency of the absorption refrigeration i in the scene s at the time t;

The Waste Heat Boiler in the paper is primarily used for the absorption and utilization of waste heat from micro gas turbines for heating purposes. The other waste heat generated by micro turbines is directed towards the absorption refrigeration for cooling. The mathematical model for the waste heat boiler is as follows:

$$H_{i,s,t}^{\mathrm{WHB}} = \frac{P_{\mathrm{MT}}(t)}{\eta_{i,s,t}^{\mathrm{MT}}} \cdot \xi_{i,s,t}^{\mathrm{WHB}} (1-\eta_{i,s,t}^{\mathrm{MT}} - \eta_l) \cdot COP_{i,s,t}^{\mathrm{WHB}} \tag{2-20}$$

Where $H_{i,s,t}^{\mathrm{WHB}}$ —— heat generation of waste heat boiler i in the scene s at the time t;

$\xi_{i,s,t}^{\mathrm{WHB}}$ —— proportion of waste heat obtained by waste heat boiler i in the scene s at the time t;

η_l —— the loss of waste heat during the transmission process;

$COP_{i,s,t}^{\mathrm{WHB}}$ —— efficiency of waste heat boiler i in the scene s at the time t;

The heat pump system consists of electric heat pump and electrical chiller. Mathematical model of the electrical chiller is as follows:

$$Q_{i,s,t}^{\mathrm{EC}} = P_{i,s,t}^{\mathrm{EC}} \cdot COP_{i,s,t}^{\mathrm{EC}} \tag{2-21}$$

Where $Q_{i,s,t}^{\mathrm{EC}}$ —— cooling power of electrical chiller i at scene s time t;

$P_{i,s,t}^{\mathrm{EC}}$ —— electricity consuming of electrical chiller i at scene s time t;

$COP_{i,s,t}^{\mathrm{EC}}$ —— cooling efficiency of electrical chiller i at scene s time t;

Mathematical model of the electrical heat pump is as follows:

$$H_{i,s,t}^{\mathrm{EHP}} = P_{i,s,t}^{\mathrm{EHP}} \cdot COP_{i,s,t}^{\mathrm{EHP}} \tag{2-22}$$

Where $H_{i,s,t}^{\mathrm{EHP}}$ —— heating power of electrical heat pump i at scene s time t;

$P_{i,s,t}^{\mathrm{EHP}}$ —— electricity consuming of electrical heat pump i at scene s time t;

$COP_{i,s,t}^{\mathrm{EHP}}$ —— cooling efficiency of electrical heat pump i at scene s time t;

The distributed energy system consists of wind power system and photovoltage system. The relationship between the actual power output of a wind turbine $P_{i,s,t}^{wt}$ and the actual wind speed can be represented as:

$$P_{i,s,t}^{\mathrm{wt}}=\begin{cases}0 & v_{i,s,t}<v_{ci}\\ k_1 v_{i,s,t}+k_2 & v_{ci}<v_{i,s,t}<v_r\\ P_r & v_{i,s,t}>v_r\end{cases} \tag{2-23}$$

Where $P_{i,s,t}^{\mathrm{wt}}$ —— power generation of the wind turbine i at scene s time t;

$v_{i,s,t}$ —— the actual wind speed around of the wind turbine i at scene s time t;

v_{ci}、v_r —— the cut-in and cut-out wind speeds of the wind turbine;

P_r —— rated power of the wind turbine;

To model the actual performance of photovoltaic (PV) power generation, the equation for PV power generation is as follows:

$$P_{i,s,t}^{\mathrm{pv}}=A_{i,s,t}^{\mathrm{pv}}\times\eta_{s,t}^{\mathrm{pv}}\times SRI_{s,t} \tag{2-24}$$

Where $P_{i,s,t}^{\mathrm{pv}}$ —— power generation of PV i at scene s time t;

$A_{i,s,t}^{\mathrm{pv}}$ —— actual generating area of PV i at scene s time t;

$\eta_{s,t}^{\mathrm{pv}}$ —— generation efficiency of PV i at scene s time t;

$SRI_{s,t}$ —— solar radiation index on the PV i at scene s time t;

The detailed power generation efficiency $\eta_{s,t}^{pv}$ for the PV i at scene s time, can be expressed as:

$$\eta_{s,t}^{\mathrm{pv}}=P_1\cdot\left[\left(\frac{SRI_{s,t}}{SRI_0}\right)^{P_2}+P_3\left(\frac{SRI_{s,t}}{SRI_0}\right)\right]\left[1+P_4\left(\frac{T_{s,t}}{T_0}\right)+P_5\frac{AM_{s,t}}{AM_0}\right] \tag{2-25}$$

Where SRI_0 —— reference solar radiation index for the PV panel;

T_0 —— reference environmental temperature for the PV panel;

$T_{s,t}$ —— environmental temperature at scene s time t;

$AM_{s,t}$ —— air quality at scene s time t;

AM_0 —— reference environmental air quality at scene s time t;

P_1、P_2、P_3、P_4、P_5 —— fixed parameters in the formula;

Energy storage systems mainly include battery storage and heating storage, which can store electrical and heating, respectively. The energy storage systems release energy at appropriate times to effectively reduce fluctuations in device outputs within the system. At any given moment, a battery can only charge or discharge. The actual energy of the battery $E_{i,s,t}^{ba}$ at the current time, depends on the previous energy the battery E_{i,s,t_0}^{ba}, and the charging and discharging power within that time period. The

specific formula is as follows:

$$E_{i,s,t}^{ba} = E_{i,s,t_0}^{ba} + \eta_{i,s,t}^{ba\_in} E_{i,s,t}^{ba\_in} - \eta_{i,s,t}^{ba\_out} E_{i,s,t}^{ba\_out} \tag{2-26}$$

In the formula $E_{i,s,t}^{ba}$ —— actual energy of battery i at scene s time t;

E_{i,s,t_0}^{ba} —— actual energy of battery i at scene s time t_0;

$\eta_{i,s,t}^{ba\_in}$ —— charging efficiency of battery i at scene s time t;

$E_{i,s,t}^{ba\_in}$ —— charging electricity of battery i at scene s time t;

$\eta_{i,s,t}^{ba\_out}$ —— discharging efficiency of battery i at scene s time t;

$E_{i,s,t}^{ba\_out}$ —— discharging electricity of battery i at scene s time t;

Charging and discharging process are constrained by the following equations：

$$0 \le E_{i,s,t}^{ba\_in} \le Bi_{i,s,t}^{ba\_in} \cdot E_{ba\_in}^{\lim it} \tag{2-27}$$

where $Bi_{i,s,t}^{ba\_in}$ —— charging binary of battery i at scene s time t;

$E_{ba\_in}^{\lim it}$ —— maximum charging capacity of battery;

$$0 \le E_{i,s,t}^{ba\_out} \le Bi_{i,s,t}^{ba\_out} \cdot E_{ba\_out}^{\lim it} \tag{2-28}$$

where $Bi_{i,s,t}^{ba\_out}$ —— discharging binary of battery i at scene s time t;

$E_{ba\_out}^{\lim it}$ —— maximum discharging capacity of battery;

$Bi_{i,s,t}^{ba\_in}$, $Bi_{i,s,t}^{ba\_out}$ satisfy the following equation：

$$0 \le Bi_{i,s,t}^{ba\_in} + Bi_{i,s,t}^{ba\_out} \le 1 \tag{2-29}$$

$$H_{i,s,t}^{hs} = H_{i,s,t_0}^{hs} + \eta_{i,s,t}^{hs\_in} E_{i,s,t}^{hs\_in} - \eta_{i,s,t}^{hs\_out} E_{i,s,t}^{hs\_out} \tag{2-30}$$

where $H_{i,s,t}^{hs}$ —— actual heating energy of heating storage i at scene s time t;

H_{i,s,t_0}^{hs} —— actual heating energy of heating storage i at scene s time t_0;

$\eta_{i,s,t}^{hs\_in}$ —— heating storing efficiency of heating storage i at scene s time t;

$E_{i,s,t}^{hs\_in}$ —— heating storing of heating storage i at scene s time t;

$\eta_{i,s,t}^{hs\_out}$ —— heating releasing efficiency of heating storage i at scene s time t;

$E_{i,s,t}^{hs\_out}$ —— heating releasing of heating storage i at scene s time t;

Storing and releasing heating energy should satisfy the equations(2-31) and (2-32):

$$0 \le H_{i,s,t}^{hs\_in} \le Bi_{i,s,t}^{hs\_in} \cdot H_{hs\_in}^{limit} \tag{2-31}$$

where $Bi_{i,s,t}^{hs\_in}$ —— heating storing binary of heating storage i at scene s time t;

$H_{hs\_in}^{limit}$ —— maximum heating storing capacity of heating storage;

$$0 \le H_{i,s,t}^{hs\_out} \le Bi_{i,s,t}^{hs\_out} \cdot H_{hs\_out}^{limit} \tag{2-32}$$

where $Bi_{i,s,t}^{hs\_out}$ —— heating releasing binary of heating storage i at scene s time t;

$H_{hs\_out}^{limit}$ —— maximum heating releasing capacity of heating storage;

$Bi_{i,s,t}^{hs\_in}$, $Bi_{i,s,t}^{hs\_out}$ satisfy the following equation：：

$$0 \le Bi_{i,s,t}^{hs\_in} + Bi_{i,s,t}^{hs\_out} \le 1 \tag{2-33}$$

2.2.2 IES objective

The integrated energy system described in this paper primarily provides electricity, heating, and cooling services. Energy service providers construct distributed generation units, including combined heat and power (CHP) units, photovoltaic (PV) generation units, heat pump systems, and energy storage systems, within the park. The generated electricity, cooling, and heating energy are sold to customers by the energy service provider. Within the park, the energy service provider sets up distributed power sources, higher-level power sources, microgrids, energy storage units, and distribution systems for electricity, heating, and cooling. These facilities offer electricity distribution services and heating and cooling services for residential communities, industrial parks, commercial areas, and other applications. The energy service provider establishes a business operation model based on the coordination of generation, network, and load in the integrated energy system, operating in an interconnected manner for heating, cooling, and electricity. Through an energy management system, the energy service provider optimizes and coordinates the load dispatch, using flexible load scheduling methods to ensure a high level of customer satisfaction while maximizing the profit for the integrated energy system service provider.

The scheduling discussed in this paper is an elastic scheduling process within the context of the integrated energy system. Setting energy prices and controlling device output based on real-time demand can improve energy utilization efficiency and reduce

generation costs. However, in the integrated energy system, the production and conversion of heating, cooling, and electricity are not solely dependent on large-scale energy generation equipment such as wind power, solar power, natural gas, and thermal power. It is increasingly desirable to gradually replace centralized energy supply with large-scale distributed renewable energy sources. Centralized energy supply equipment serves primarily to maintain grid stability and power balance.

Therefore, in the flexible scheduling process heavily influenced by the output of a large amount of distributed renewable energy, uncertainties in energy supply and load increase significantly and are difficult to predict. As energy service providers, it is challenging to grasp and predict consumers' actual electricity consumption strategies. These factors greatly increase the difficulty for energy service providers to control and manage the integrated energy system.

Furthermore, the introduction of the consumer's cost per satisfaction index in this chapter indicates that consumers have not only price preferences but also requirements for the satisfaction of their energy needs. Therefore, unlike most papers [67] that place pricing power in the hands of the integrated energy scheduling provider and adjust the total energy consumption on the consumer side, this paper aims to safeguard the interests of consumers. It completely centralizes the supply scheduling in the hands of the integrated energy service provider, enabling the integrated energy system to more efficiently leverage the advantages of the system and giving consumers the bargaining power to share in the cost advantages of the integrated energy system. This game model transforms consumers from being solely energy consumers to becoming active participants with dual characteristics of energy consumption and negotiation. Consumers can engage in transactions and collaboratively determine the integrated energy supply price with the higher-level service providers, thereby enhancing their ability to negotiate energy consumption and reducing the operating costs of the integrated energy system.

Furthermore, the introduction of the user's energy cost satisfaction index in this chapter indicates that users not only have price preferences in actual energy consumption but also have requirements for the degree of energy satisfaction.Therefore, unlike most papers [67] that delegate the pricing authority to the integrated energy dispatchers to adjust the total user-side energy consumption, this study, in order to safeguard users' interests, centralizes the energy supply scheduling entirely with the integrated energy operators. This approach allows the integrated energy system to efficiently leverage its advantages while empowering users with the negotiation power, enabling them to share

in the cost benefits of the integrated energy system. This game-theoretic model transforms users from mere energy consumers to active participants with dual attributes of energy consumption and negotiation. Through transactions with upper-level service providers, users can collaboratively set the comprehensive energy supply price, enhancing their negotiation capabilities and reducing the operational scheduling costs of the integrated energy system.For the integrated energy service provider, the most crucial objective is to maximize profits. Under the scheduling and operational framework described in the paper, revenue primarily comes from fees charged to users. After subtracting the operational costs of the integrated energy system, the overall operational profit can be calculated using the following formula:

$$\max F = \sum_{t} [RE_t - C_t^{fd} - C_t^{wh}] \tag{2-34}$$

Due to significant variations in satisfaction and demand fluctuations among three user groups – residential communities, industrial parks, and commercial areas – fees are levied separately for each group to reflect their actual energy usage. The expression for total revenue is as follows:

$$RE_t = CE_{jm,t} + CT_{jm,t} + CE_{gy,t} + CT_{gy,t} + CE_{sy,t} + CT_{sy,t} \tag{2-35}$$

In the equation RE_t—— charges for collecting p types of energy at time point t;

$CE_{jm,t}$、$CT_{jm,t}$—— charges for electricity and heating or cooling fees collected from residential users at time point t;

$CE_{gy,t}$、$CT_{gy,t}$—— charges for electricity and heating or cooling fees collected from industrial users at time point t;

$CE_{sy,t}$、$CT_{sy,t}$—— charges for electricity and heating or cooling fees collected from commercial users at time point t;

Generation cost C_t^{fd} is primarily composed of the generation cost of micro gas turbines and the cost of external electricity purchase.

The specific calculation expression is as follows:

$$C_t^{fd} = C_{i,s,t}^{\mathrm{MT}} + P_{i,s,t}^{gr} \cdot G_t^{gr} \tag{2-36}$$

where $C_{i,s,t}^{\mathrm{MT}}$—— the gas cost of the gas turbine i in scenario s and at time point t is given by;

$P_{i,s,t}^{gr}$—— the external grid input power of the transformer i in scenario s and at time point t is represented as;

G_t^{gr} —— the purchase price of electricity for the i transformer in scenario s and at time point t is as follows;

The depreciation and maintenance costs of various devices in the integrated energy system during their usage are approximated as linear functions of the generated output, expressed as: $C_t^{wh} = \sum \theta_{i,s,t}^{\varphi} \cdot P_{i,s,t}^{\varphi}, \varphi = MT, AR, WHB, EHP, wt, pv, ba, hs$ (2-37)

where $\theta_{i,s,t}^{\varphi}$ —— the maintenance cost coefficient of the the φ device i in scenario s and at time point t is as follows;

$P_{i,s,t}^{\varphi}$ —— output power of the φ device in scenario s at time t.;

2.2.3 IES operating constraints

In the integrated energy system described in this paper, the electricity generation of the system needs to satisfy not only the user demand for power supply but also the requirements of the heat pump and energy storage systems to ensure the stability of the overall integrated energy system operation. The specific formula for the electricity load energy balance is:

$$\sum_i P_{i,t}^{E} = \sum_i P_{i,s,t}^{\mathrm{MT}} - \sum_i P_{i,s,t}^{\mathrm{EHP}} - \sum_i P_{i,s,t}^{\mathrm{EC}} + \sum_i P_{i,s,t}^{\mathrm{wt}} + \sum_i P_{i,s,t}^{\mathrm{pv}} + \sum_i E_{i,s,t}^{ba\_out} - \sum_i E_{i,s,t}^{ba\_in} + \sum_i P_{i,s,t}^{gr} \quad (2\text{-}38)$$

In addition to meeting the user's electricity demand, there is also a requirement to fulfill the user's heating demand. Within the integrated energy system, heating is primarily accomplished through electric heat pumps and waste heat recovery boilers, supplemented by thermal storage tanks for heat storage and release. The comprehensive formula for the thermal load energy balance is as follows:

$$\sum_i H_{i,t} = \sum_i H_{i,s,t}^{\mathrm{WHB}} + \sum_i H_{i,s,t}^{\mathrm{EHP}} + \sum_i E_{i,s,t}^{hs\_out} - \sum_i E_{i,s,t}^{hs\_in} \quad (2\text{-}39)$$

The cooling load demand of the integrated energy system is primarily met through the absorption chiller in the CCHP system and the electric chiller in the heat pump system. The specific formula for the cooling load energy balance is as follows:

$$\sum_i Q_{i,t} = \sum_i Q_{i,s,t}^{\mathrm{AR}} + \sum_i Q_{i,s,t}^{\mathrm{EC}} \quad (2\text{-}40)$$

In addition to the energy balance constraints, the integrated energy system must also adhere to its operational constraints. The operation of each device must remain within its inherent operational range.

$$P_{\min}^{\varphi} \le P_{i,s,t}^{\varphi} \le P_{\max}^{\varphi}, \varphi = MT, AR, WHB, EHP, wt, pv, ba, hs \tag{2-41}$$

In the formula $P_{\min}^{\varphi}$ —— the minimum value of the output power of the device φ;

$P_{\max}^{\varphi}$ —— the maximum value of the output power of the device φ;

$P_{i,s,t}^{\varphi}$ —— the output power of the φ device i in scenario s at time point t;

Furthermore, specific operational constraints of the devices are detailed in Section 2.2.2, Device Model, and will not be reiterated here.

2.3 Summary

This chapter begins by introducing the method for calculating user thermal comfort and proposes the thermal comfort satisfaction index based on this calculation. Additionally, the relationship between indoor temperature and thermal comfort satisfaction is established through a series of relevant functions related to indoor temperature. By applying formulas related to heat transfer, the changes in indoor temperature resulting from the combined effects of outdoor temperature variations and the heating and cooling supplied by the integrated energy system are derived. As a result, this chapter establishes a connection between the scheduling of energy supply in the integrated energy system and user thermal comfort satisfaction.

Furthermore, the chapter introduces the concept of electricity satisfaction based on relevant literature and combines it with formulas related to unit cost satisfaction. The chapter proposes a user benefit objective function that integrates electricity satisfaction and thermal comfort satisfaction under certain supply cost and temperature regulation cost conditions. Additionally, the chapter develops mathematical models for the devices within the integrated energy system, including the CCHP (combined cooling, heating, and power) system, heat pump system, distributed energy generation system, and energy storage system. The chapter establishes operational constraints for the devices in the integrated energy system based on the studied mathematical models and combines them with energy balance constraints that account for user energy consumption patterns.

In addition, the chapter formulates the operational goals of the integrated energy

system and their corresponding mathematical models. It presents a mathematical model for user elastic load and the load scheduling of the integrated energy system, thereby providing the foundation for the subsequent game theory model in the next chapter.

3 Game-based flexible load dispatch

Building upon the integrated energy user energy utility model and system operation model established in Chapter 2, this chapter introduces a method for elastic load scheduling. The primary goal of this method is to maximize the operational benefits of the integrated energy system while simultaneously optimizing user energy utility. This is achieved by identifying a game equilibrium that strikes a balance between these two objectives, leading to an optimal scheduling of the integrated energy system's operations.

3.1 Flexible load dispatch model

In the practical scheduling of integrated energy systems, the costs and profits are primarily borne by the entity responsible for operating the system, which we'll refer to as the Integrated Energy System Scheduling Service Provider.

Due to the frequent occurrence of multiple peak load demands in the actual operation of the integrated energy system, external electricity costs tend to be high during such periods. The energy storage systems within the system, which are used to alleviate energy demand peaks, might not be able to provide sufficient reserve energy (especially if lacking cooling energy storage equipment). Hence, implementing a certain level of elastic load mechanism during peak periods can be beneficial. For instance, during a heating demand peak, a portion of the load of user groups with lower satisfaction demands could be reduced. Specifically, during the daytime working peak, commercial establishments might be willing to pay more to maintain suitable temperatures, whereas many residential properties might remain unoccupied, leading to less willingness to spend on heating. Redirecting more heating energy towards commercial establishments while slightly decreasing the heating load for residential

users can significantly relieve the pressure on the integrated energy system scheduling and reduce energy supply costs. Since commercial communities are willing to pay more at such times, and the integrated energy system scheduling service provider also experiences cost reduction, the optimization principle of maximizing the target function encourages compensation for users. In the practical implementation of elastic load scheduling, the specific mathematical expression is as follows:

Before the introduction of elastic load scheduling, the integrated energy system scheduling service provider must meet all users' electricity, heating, and cooling load demands. At this point, the user's utility function for unit cost satisfaction is given by:

$$SA_{i,t}^{\ 0} = \frac{PES_{i,t}^{\ 0}}{CE_{i,t}^{\ 0}} \cdot \frac{PTS_{i,t}^{\ 0}}{CT_{i,t}^{\ 0}} \tag{3-1}$$

where $SA_{i,t}^{\ 0}$—— initial unit energy satisfaction percentage of the user group i at time point t;

$CE_{i,t}^{\ 0}$—— initial total cost of electricity consumption for the user group i at time point t;

$CT_{i,t}^{\ 0}$—— initial total cost of cooling or heating for the user group i at time point t;

$PTS_{i,t}^{\ 0}$—— initial satisfaction percentage of electricity energy consumption for the user group i at time point t;

At this stage, the initial electricity cost paid by user groups is calculated based on the electricity consumption and the actual electricity price. The specific expression is as follows:

$$CE_{i,t}^{\ 0} = P_{i,t}^{E} \cdot J_{i,t}^{E} \tag{3-2}$$

where $J_{i,t}^{E}$—— unit electricity price for the user group i at time point t;

Similarly, the initial cooling or heating cost paid by user groups is also calculated based on the cooling or heating consumption. The specific expression is as follows:

$$CT_{i,t}^{\ 0} = H_{i,t} \cdot J_{i,t}^{H} + Q_{i,t} \cdot J_{i,t}^{Q} \tag{3-3}$$

where $J_{i,t}^{H}$ —— unit heating price for the user group i at time point t;

$J_{i,t}^{Q}$ —— unit cooling price for the user group i at time point t;

During the cooling and heating load elasticity scheduling, the user's temperature satisfaction decreases, leading to a corresponding decrease in the temperature cost they are willing to pay. At the same time, it is necessary to ensure that the unit cost satisfaction utility function value of users at this point is not less than the initial unit cost satisfaction utility function value. This ensures that users are willing to accept the energy system operator's elastic load scheduling scheme. The formula can be expressed as follows:

$$\begin{cases} SA_{i,t}^{'} = \dfrac{PES_{i,t}}{CE_{i,t}} \cdot \dfrac{PTS_{i,t}^{'}}{CT_{i,t}^{'}} \\ SA_{i,t}^{'} \geq SA_{i,t}^{0} \\ PTS_{i,t}^{'} < PTS_{i,t}^{0} \\ CT_{i,t}^{'} < CT_{i,t}^{0} \end{cases} \tag{3-4}$$

In the formula $SA_{i,t}^{'}$ —— unit thermal comfort satisfaction percentage for the user group i after the scheduling of thermal flexibility at time point t;

$CT_{i,t}^{'}$ —— total initial cost for cooling or heating for the user group i after the scheduling of thermal flexibility at time point t;

$PTS_{i,t}^{'}$ —— percentage of thermal energy satisfaction for cooling or heating for the user group i after the scheduling of thermal flexibility at time point t;

During the electricity load elasticity scheduling, the user's electricity satisfaction decreases, resulting in a corresponding decrease in the electricity cost they are willing to pay. It is also necessary to ensure that the unit cost satisfaction utility function value of users at this point is not less than the initial unit cost satisfaction utility function value. This ensures that users are willing to accept the energy system operator's elastic load scheduling scheme. The formula can be expressed as follows:

$$\begin{cases} SA_{i,t}^{"} = \dfrac{PES_{i,t}^{"}}{CE_{i,t}^{"}} \cdot \dfrac{PTS_{i,t}^{0}}{CT_{i,t}^{0}} \\ SA_{i,t}^{"} \geq SA_{i,t}^{0} \\ PES_{i,t}^{"} < PES_{i,t}^{0} \\ CE_{i,t}^{"} < CE_{i,t}^{0} \end{cases} \tag{3-5}$$

In the formula $SA_{i,t}^{"}$—— percentage of electricity energy satisfaction for the user group i after the scheduling of electricity demand flexibility at time point t;

$CE_{i,t}^{"}$—— total cost of electricity consumption for the user group i after the scheduling of electricity demand flexibility at time point t;

$PES_{i,t}^{"}$ —— initial satisfaction percentage of electricity and energy consumption for the user group i after the scheduling of electricity demand flexibility at time point t;

3.2 Stackelberg game model

3.2.1 Brief introduction

The Stackelberg game (also known as the leader-follower game) is a game theory concept in economics where participants engage in a game where a leader acts first, followed by the followers. In the traditional Stackelberg game, participants include a leader and a single follower, and they compete in terms of quantities. The leader in a Stackelberg game is sometimes referred to as the market leader. Additionally, many scholars have extended this concept to create a one-leader, multiple-follower Stackelberg game.

There are several constraints and conditions to maintain equilibrium in this game. The leader must know the follower's reaction to its action in advance. The follower must not have a way to commit to a future action that is not Stackelberg. The leader must be aware of this. In fact, if followers could commit to a non-Stackelberg action by the

leader and the leader knows this, then the leader's best response would be to play the action of a Stackelberg follower.

If a firm has some advantage that allows it to act first, then that firm might engage in Stackelberg competition. More generally, the leader must have commitment power. Observable first-mover advantage is the most obvious commitment device: once the leader has made the move, it cannot take it back, and it is committed to that action. If the leader is the incumbent monopolist in the industry and the follower is an entrant, then a first-mover advantage is likely.

For the detailed mathematical expressions, please provide more context or specify the specific equations you would like me to elaborate on.

$$\begin{cases} \min F(x, \bar{y}) \\ s.t.\ G(x, \bar{y}) \le 0 \\ H(x, \bar{y}) = 0 \\ \bar{y} \in S(x) \end{cases} leader \tag{3-6}$$

Where x represents the decision of the leader, and y^i represents the decision of follower i. $\bar{y}^i$ is the equilibrium solution of the lower-level game model. The mathematical expression is as follows:

$$\begin{cases} \bar{y}^i = arg \min f_i(x, y^i, y^{-i}) \\ s.t.\ g_i(x, y^i) \le 0 \\ h_i(x, y^i) = 0 \end{cases} \quad follower: \forall i \tag{3-7}$$

From the above mathematical model, it can be deduced that when the upper-level strategy is fixed, and the lower-level game satisfies convexity conditions for both the objective function and constraints, there exists a unique equilibrium solution. The upper-level game's objective function is only related to the leader's strategy and the equilibrium solution of the lower-level game. Solving the model involves first finding the strategy set for follower's profit maximization, which is the lower-level game, and

then plugging the follower's production response into the leader's maximum revenue function to determine the leader's strategy.

In summary, given a fixed upper-level strategy, the lower-level game is solved by maximizing the follower's profit subject to the given constraints. Once the follower's optimal strategy set is determined, it is used to calculate the leader's maximum revenue function. Then, the leader's strategy is determined by maximizing this revenue function. If you need more specific explanations or equations related to this process, please provide additional context or details.

3.2.2 Flexible load dispatch based on Stackelberg game

Based on the analysis from the previous chapter, it is evident that there exist distinct strategies and profit objectives between the Comprehensive Energy System Dispatch Service Provider and different user groups. Drawing upon the principles of leader-follower games, this paper establishes a leader-follower game scheduling model tailored for the Comprehensive Energy System Dispatch Service Provider and diverse user groups.

Given that the Comprehensive Energy System Dispatch Service Provider holds a dominant position in energy scheduling and proactively engages in elastic load scheduling based on its operational status and user energy supply demands, while users primarily adjust their payment strategies according to the provider's scheduling decisions, it is logical to designate the Comprehensive Energy System Dispatch Service Provider as the leader. As for users, since residential communities, industrial parks, and commercial districts vary in terms of satisfaction, energy demands at different times, and their willingness to pay, they are divided into three distinct user groups and treated as followers. The specific structure is illustrated in Figure 3-1.

Please let me know if you need further clarification or assistance.

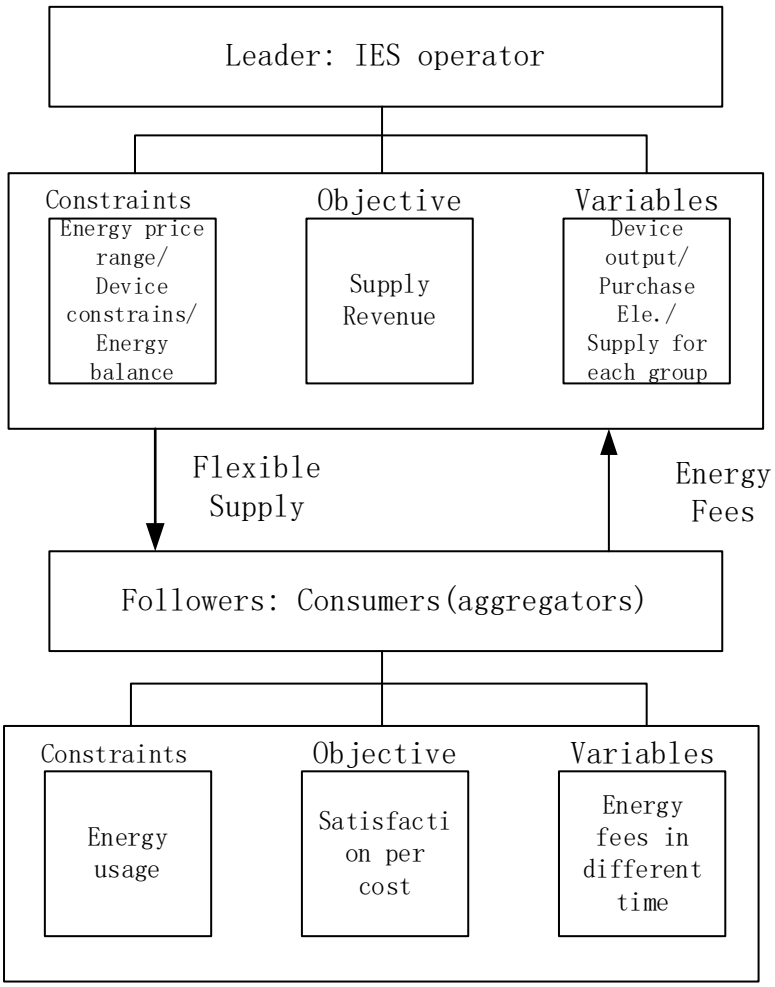

Figure 3-1 Elastic Load Dispatch Game Model

Unlike the majority of papers that employ price regulation [58-62], the Comprehensive Energy System Dispatch Service Provider in this study adjusts energy prices based on the received load information, aiming to balance its interests while ensuring user satisfaction with energy usage. In the context of optimizing the comprehensive energy dispatch, the Comprehensive Energy System Dispatch Service Provider engages in a price-game interaction with users. By guaranteeing both the optimization of the energy dispatch and user satisfaction, the goal is to reduce the overall energy cost for users.

The energy service provider dynamically adjusts its dispatch strategy based on the price strategies of the underlying users, while users adapt their payment strategies according to the continually evolving supply effect provided by the service provider.

Through iterative strategy optimization, the energy service provider's energy dispatch strategy and user payment prices reach a dynamic equilibrium, known as a Nash equilibrium solution.

The fundamental components of the game model include participants, strategies, and payoffs. The game can be described as follows:

Please let me know if you need further assistance or any specific details.

$$G=\begin{Bmatrix}\{IER\cup users\};\\ \{\rho_{IER}\};\{C_{users}\};\\ F;SA_{users}\end{Bmatrix} \tag{3-8}$$

（1） The participants include the integrated energy retailer (IER) providing comprehensive energy system scheduling services, and three user groups - residential users, commercial users, and industrial users. The set of users can be represented as $users=\{user\_jm\cup user\_gy\cup user\_sy\}$, thus the set of participants can be represented as $\{IER\cup users\}$.

（2） The strategies include the equipment output and comprehensive energy allocation policies formulated by the integrated energy system scheduling provider. These output and allocation policies can be represented as set $\{\rho_{IER}\}$. On the other hand, the energy prices proposed by users in response to the comprehensive energy scheduling supply situation can be represented as set $\{C_{users}\}$. This refers to the electricity prices for residential, commercial, and industrial users, as well as the heating and cooling energy prices for maintaining indoor temperatures.

（3） The benefits consist of the revenue for the energy service provider, denoted as F, and the benefits for the users, denoted as $SA_{users}=\{SA_{jm},SA_{sy},SA_{gy}\}$.

3.2.3 Game equilibrium verification

In the master-slave game model, the leader (or leader firm) makes decisions based on its own interests without knowing the strategies of the other followers. The followers (or follower firms) respond optimally to the leader's strategy without knowing the strategies of the other followers. The leader then dynamically adjusts its strategy based on the responses of the followers. This process continues until an equilibrium solution is reached. The fundamental components of the master-slave game include participants, strategies, and payoffs.

When solving a master-slave game, the first step is to prove the existence and uniqueness of its Nash equilibrium solution. Both the leader energy service provider and the follower users aim to maximize their respective payoffs by employing specific optimization strategies. In the equilibrium solution, the pricing strategies for all users correspond to the optimal load dispatch (device outputs and energy allocation) by the comprehensive energy system dispatch service provider. Likewise, the load dispatch strategy of the service provider corresponds to the optimal pricing strategies for all users. In this equilibrium solution, neither the energy service provider nor the users can unilaterally change their strategies to achieve greater payoffs.

In this situation, if there exists a set of strategy pairs $(\rho_{IES}^{*}, C_{users}^{*})$ for both upper and lower levels that satisfy the condition where the comprehensive energy system dispatch service provider's leader's equipment output and integrated energy allocation strategy correspond to ρ_{IES}^{*}, such that all followers accept the pricing arrangement in response to following the strategies of the comprehensive energy system dispatch service provider's leader, then $(\rho_{IES}^{*}, C_{users}^{*})$ represents the desired equilibrium solution for the leader-follower game. In this case, the strategy set $(\rho_{IES}^{*}, C_{users}^{*})$ satisfies the following conditions:

$$\begin{cases} F(\rho_{IES}^{*}, C_{users}^{*}) \geq F(\rho_{IES}, C_{users}) \\ SA_{users}(\rho_{IES}^{*}, C_{users}^{*}) \geq SA_{users}(\rho_{IES}, C_{users}) \end{cases} \tag{3-9}$$

Once the strategy sets and outcomes as mentioned above are obtained, both the leader and followers lack the incentive to change their strategies. As a result, achieving a balance in the game, known as Nash equilibrium, becomes feasible. Before solving for the equilibrium solution of the Stackelberg game, we can apply the theorem that confirms the existence of Stackelberg equilibrium to validate the existence of Nash equilibrium solution in the proposed master-slave game model.

When the following conditions are met, the equilibrium solution for the proposed game setting exists:

1、The strategy sets of the leader and followers are non-empty and compact convex sets.;

2 、Given the leader's strategy, each follower has a unique optimal strategy for their objective function.

3 、Given the followers' strategies, the leader also has a unique optimal strategy.

Considering the model presented in this paper, the satisfaction of these three conditions can be explained as follows:

1、 According to the comprehensive energy dispatch system model discussed in the previous chapter, it is evident that the strategies of the comprehensive energy system dispatch service provider's leader satisfy equations (2-16) to (2-40). Equations (2-21), (2-22), (2-23), (2-26), (2-30), (2-38), (2-39), and (2-40) represent linear functions, while the remaining equations are convex functions. For the strategies of the users, they need to satisfy equations (3-4) and (3-5), which are also non-empty and strictly convex functions. Therefore, the leader and follower strategy sets proposed in this paper for the leader-follower game model are both non-empty and strictly convex.

2、 This point requires proof that when the strategy of the comprehensive energy system dispatch service provider (leader) is determined, the strategies of the follower users are also determined.

For the users' unit cost satisfaction objective function, when the strategies of the comprehensive energy system dispatch service provider's leader ρ_{IES}^{*} are determined, according to equations (2-38) and (2-10), the electricity satisfaction $PES_{i,t}$ can be computed. Simultaneously, when the dispatch strategies of the leader of the comprehensive energy system dispatch service provider are determined, the cooling and heating amounts obtained by the user followers are also uniquely determined. Considering the outdoor temperature and the previous indoor temperature, the real-time indoor temperature can be calculated using equation (2-7), and the user's thermal comfort can be obtained through equations (2-8) and (2-9), thus calculating the thermal

comfort satisfaction percentage $PTS_{i,t}$ of the user group i at time point t. Therefore, in the equations, $PES_{i,t}$ and $PTS_{i,t}$ are constants at this point. The expression of $SA_{i,t}$ is a strictly quasi-convex function[67] because an optimal solution must exist

3、 This point needs to prove that when the payment strategies of follower users are determined, the strategy of the leader, the comprehensive energy system dispatch service provider, can also be determined.

For the leader of the comprehensive energy system dispatch service provider's profit objective function, when the follower users' payment strategies $C_{users}=\{CE_{i,t},CT_{i,t}\}$ are determined, according to equation (2-35), the revenue of the leader of the comprehensive energy system dispatch service provider can be determined. Simultaneously, since the leader of the comprehensive energy system dispatch service provider can know the heating and cooling demands of users calculated according to equation (2-7), as well as the electricity demand obtained through user electricity predictions, they can formulate dispatch strategies based on the equipment operation equations and constraints from equations (2-16) to (2-40). Considering that the cost functions C_t^{fd} and C_t^{wh} in the objective function are convex functions with respect to equipment outputs, the total objective function F is also a convex function with respect to equipment outputs. Hence, there must exist an optimal solution.

3.3 Algorithm and process

3.3.1 GBO

In optimization problems, Graph Based Optimization (GBO) is particularly suitable for representing optimization problems involving discrete-time dynamic systems within a finite time horizon. It utilizes a natural block structure encoded by sparsely connected hypergraphs to handle optimization problems [68]. In practical optimization scenarios, the abstract structure of a graph is used to represent real-world problems, where nodes represent optimization subproblems, and hyperedges represent relationships between nodes. Graph-based optimization modeling defines a common global discretized time range shared by all nodes, along with associated time intervals, allowing optimization to be carried out within specific time ranges. This approach is particularly suitable for optimization problems with a large number of variables changing over time. Each optimization node has internal and external (or coupled) variables, and internal constraints can be defined within each node, along with local

objective functions representing their contribution to the system-wide objectives. Finally, for each hyperedge, constraint relationships between different nodes are established through coupled variables.

Let $G=(N,\varepsilon)$ be a hypergraph representing the block-structured optimization problem to be addressed, with a node set N and a hyperedge set $\varepsilon \subseteq 2^N$ (where each hyperedge corresponds to a subset of nodes). Let T be the considered time range, and let $T=0$, $T=\{0,1,\ldots,T-1\}$ is a set of time components relevant to this optimization problem.

Let $x^n \in X^n$ and $z^n \in Z^n$ denote the sets of internal variables and coupling variables defined at node $n \in N$. These variables can take values from either discrete or continuous sets. Additionally, for any hyperedge $e \in \varepsilon$, let $Z^e = \{Z^n \mid n \in e\}$ represent the set of coupling variables mutually associated within each node connected to that hyperedge.

For the optimization objective of a specific node, let F^n represent the function defining the local objective at node n. Building upon this, consider the following form of scalar objective:

$$F^n(X^n,Z^n) = f_0^n(X^n,Z^n) + \sum_{t\in T} f^n(X^n,Z^n,t) \tag{3-10}$$

where f_0^n—— scalar affine functions with respect to X^n and Z^n that do not involve time variables.;

f^n—— scalar affine functions with time variables related to X^n and Z^n;

F^n——function defining the local objective at node n;

Both equality and inequality constraints can be defined at each node. More precisely, an arbitrary number of constraints can be defined, and each constraint can be extended over a subset of time intervals. Therefore, we can consider the following form of equality constraints:

$$h_k^n(X^n,Z^n,t) = 0, \forall t \in T_k^n \tag{3-11}$$

where h_k^n—— scalar affine function concerning X^n and Z^n, as well as any time variable $T_k^n \subseteq T$ within the time series t;

Simultaneously, inequality constraints can also be defined at each node n, and

the expressions are as follows:：

$$g_k^n(X^n, Z^n, t) \le 0, \forall t \in T_k^n \tag{3-12}$$

where g_k^n—— scalar affine functions with respect to X^n and Z^n, as well as any time variable t in the time sequence $T_k^n \subseteq T$, can be expressed as follows;

Similarly, equality and inequality constraints can be defined on any hyperedge $e \in \varepsilon$. However, constraints can only involve the nodes associated with hyperedge $e \in \varepsilon$, which corresponds to the coupling variables of the nodes in set $n \in e$. More precisely, let H^e and G^e be affine functions of Z^e used to define equality and inequality constraints associated with hyperedge $e \in \varepsilon$. Using this notation, the types of problems that can be represented within this framework are as follows:

$$\begin{aligned} &\min \sum\nolimits_{n \in N} F^n(X^n, Z^n) \\ &s.t \quad \mathrm{h}_k^n(X^n, Z^n, t) = 0, \forall t \in T_k^n \\ &\qquad g_k^n(X^n, Z^n, t) \le 0, \forall t \in T_k^n \\ &\qquad H^e(Z^e) = 0, \forall e \in \varepsilon \\ &\qquad G^e(Z^e) \le 0, \forall e \in \varepsilon \\ &\qquad x^n \in X^n, z^n \in Z^n, \forall n \in N \end{aligned} \tag{3-13}$$

For the above formulas, let's use a hypothetical problem for a graphical representation using a block structure with four nodes (denoted as $N = \{n1, n2, n3, n4\}$) and two hyperedges (denoted as $e1 = \{n1, n2\}$ $e2 = \{n2, n3, n4\}$). As illustrated in Figure 3-2 below, among the four nodes, there is a hyperedge $e1$ between node $n1$ and node $n2$, which corresponds to mutual coupling variable constraints $H^{e1}(Z^{n1}, Z^{n2}) = 0$ between these two nodes. Similarly, there is a hyperedge $e2$ between node $n2$, node $n3$, and node $n4$, and $e2$ corresponds to mutual coupling variable constraints among these three nodes

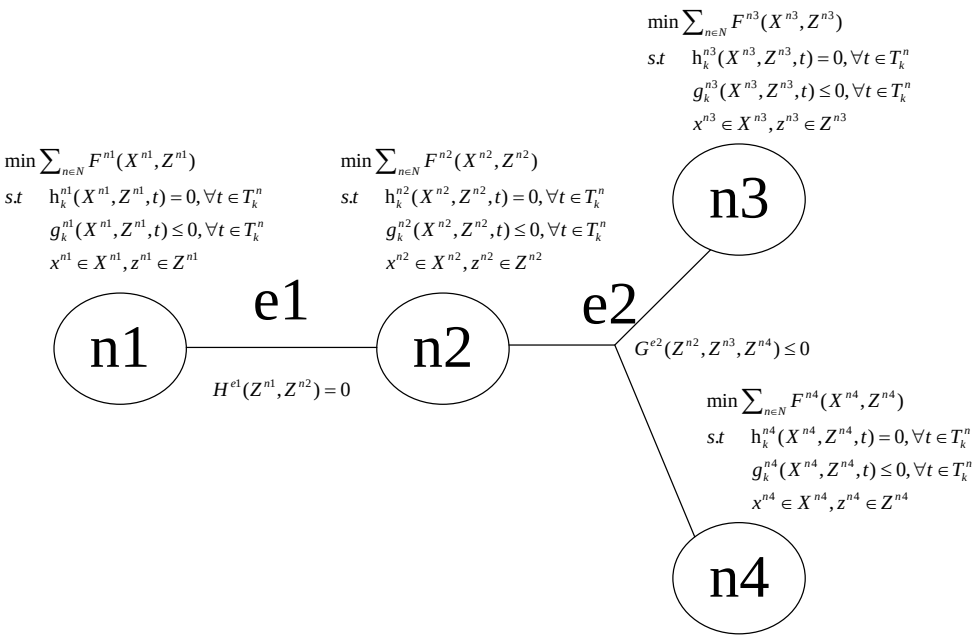

Figure 3-2 GBO Case Model

As described in the introduction to GBO, it is evident that GBO is well-suited for handling optimization problems with nodes containing different objective functions and coupled variable constraints. In the context of the proposed game model in this paper, combining it with Figure 3-2, the comprehensive energy system scheduling service provider can be represented as a distinct node, while the three types of users—residential, commercial, and industrial users—can be represented as three separate nodes. The connections between the residential, commercial, and industrial users nodes and the comprehensive energy system scheduling service provider node, as well as the coupling variable constraints, are represented through hyperedges, illustrating the balance between scheduling and payment demands, as shown in Figure 3-1.

3.3.2 Process

During the actual solving process, as depicted in the diagram Figure 3-3, the following steps are taken. Firstly, input the operational parameters of various devices within the comprehensive energy system, along with predictions of the distributed generation system output based on weather and other factors. Next, input user-related information, including the parameters of thermal comfort satisfaction equations for different users, the indoor and outdoor temperatures for the day of scheduling, and potential electricity demands of the users.

Subsequently, employing the graph-based optimization (GBO) algorithm in accordance with the master-subordinate game model established in section 3.2, the solution process begins. Starting with an initial schedule, which represents the scenario without elastic scheduling, the process then proceeds with elastic scheduling game

considering the differing utility objective functions of the comprehensive energy system scheduling service provider and the users. Once the game achieves an equilibrium solution, the result of the elastic load scheduling can be obtained.

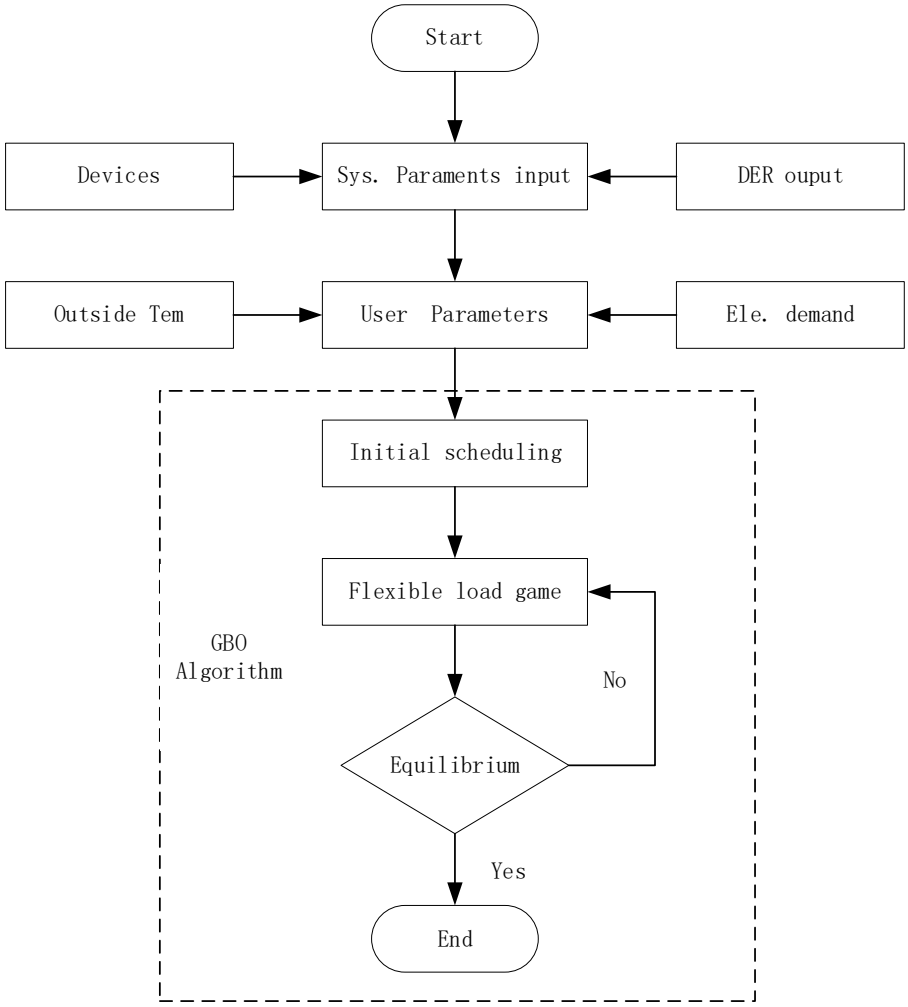

Figure 3-3 Elastic load scheduling game computation process

3.4 Summary

This chapter presents an elastic load scheduling method based on master-subordinate game theory, and it provides an overview from three perspectives: the elastic load scheduling model, the master-subordinate game model, and the implementation algorithm. Through the mathematical model outlined in section 3.1, the elastic load scheduling model establishes the dynamics of user payments, energy consumption, and utility functions during practical scheduling scenarios.

Subsequently, in section 3.2, the construction of the master-subordinate game model outlines the framework for implementing the elastic load scheduling. It also establishes the existence of equilibrium solutions. Finally, section 3.3 introduces the Graph-Based

Optimization (GBO) algorithm and outlines the process of solving the elastic load scheduling based on master-subordinate game theory using GBO.

4 Case study

4.1 System paremeters

To validate the effectiveness of the elastic load scheduling model based on master-subordinate game theory, this study considers a set of adjacent residential, commercial, and industrial communities located in Beijing as the users of the integrated energy system. The electricity demand profiles for these three types of users are illustrated in Figures 4-1, 4-2, and 4-3 respectively:

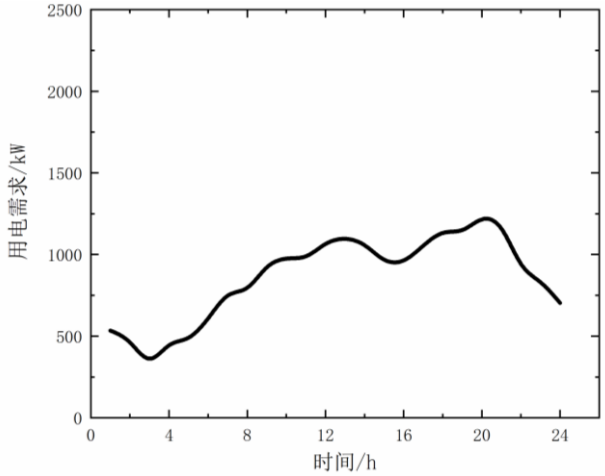

Figure 4-1 Residential electricity demand

The electricity demand peak for the residential community is mainly concentrated around noon and during the evening hours until bedtime. During the noon hours, the electricity demand is around 1000 kW, while it can reach approximately 1200 kW during the evening to bedtime period. For most other time periods, the electricity demand remains below 1000 kW. The lowest electricity demand for the residential community occurs during the early morning hours, at less than 500 kW.

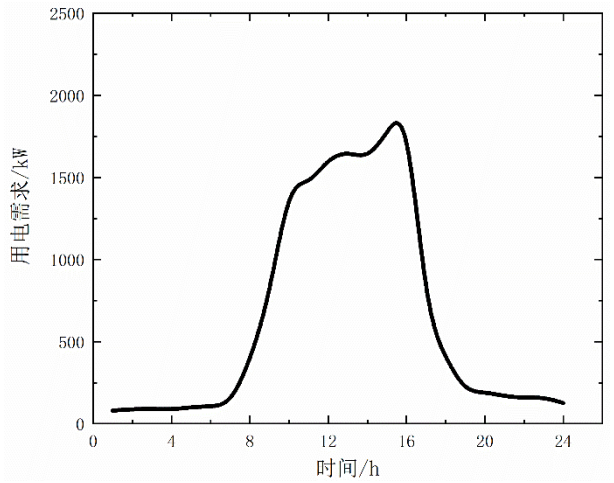

Figure 4-2 Industrial electricity demand

The industrial user's electricity consumption is concentrated during the working hours from 8 AM to 5 PM, ranging between 1500 kW and 1700 kW. During the post-work hours, there is almost no electricity demand.

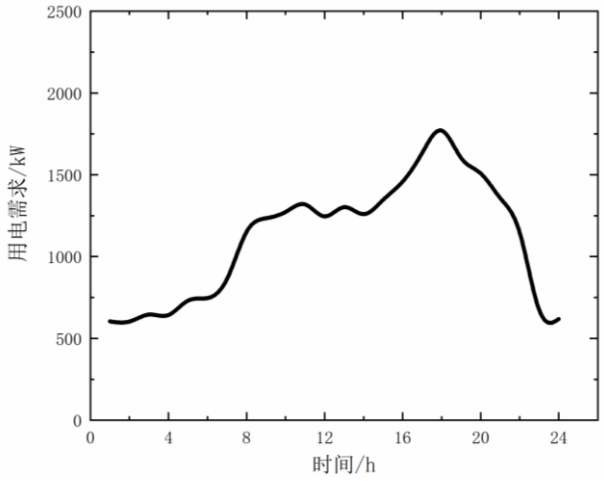

Figure 4-3 Commercial electricity demand

The electricity demand for commercial users is primarily concentrated during business hours, from 8 AM to 10 PM, with electricity demand exceeding 1000 kW. Particularly during the peak hours from 5 PM to 8 PM, the electricity consumption can reach around 1700 kW.

Overall, both industrial and commercial users exhibit significant variations in electricity demand between peak and off-peak periods. Additionally, the peak electricity demand of commercial areas can overlap with the peak demand of residential users, and when combined with the winter heating peak, it can put substantial pressure on the comprehensive energy supply load.

For the various integrated energy devices established in Section 2.2.3 of this paper, including micro gas turbines, waste heat boilers, absorption chillers, electric heat pumps, electric refrigeration machines, and energy storage devices, the following table presents some parameters of these devices, as detailed in Table 4-1.

Table 4-1 Device Parameter Table

Devices	Rated Power/Capacity (kW)	Maintenance Cost (yuan/kW)	Efficiency
Gas Turbine	5000	0.03	0.73
Electric Heat Pump	1500	0.02	2
Absorption Chiller	2000	0.015	2.5
Electric Refrigeration	2000	0.015	2.5
Waste Heat Boiler	1000	0.02	1.5
Energy Storage	3000	0.01	0.95
Thermal Storage	4000	0.005	0.98

The output curves of the photovoltaic and wind power generation systems involved in this paper are shown in Figure 4-4. The natural gas price R_{gas} used for the micro gas turbine is 0.24 yuan/m3, with an average calorific value of 9.2 kW·h/m3. The heating price of the integrated energy system is 0.5 yuan/kW·h, the cooling price is 0.58 yuan/kW·h, and the electricity price is 0.7 yuan/kW·h. The external electricity purchase price for the integrated energy system is based on a tiered pricing structure, as shown in the graph in Figure 4-4.

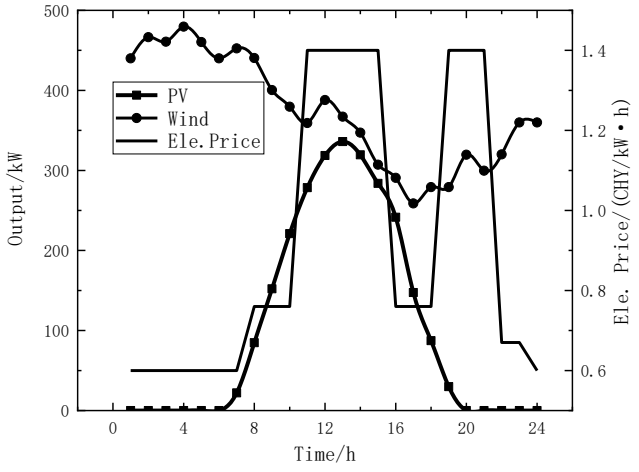

Figure 4-4 Photovoltaic (PV) power output, wind power output, and external electricity purchase prices

Simultaneously, Figure 4-4 also includes the output profiles of the wind power system and the photovoltaic system within the distributed generation system over the course of a day.

Based on the user energy consumption thermal comfort satisfaction model in section 2.1 and the formula for indoor temperature variation, it's evident that outdoor temperature directly affects the heating and cooling capacity of the integrated energy system. In this paper, we intend to examine the climate of three typical days in Beijing, corresponding to typical summer temperatures, typical winter temperatures, and typical spring and autumn temperatures. The temperature variation for these scenarios is depicted in the graph in Figure 4-5.

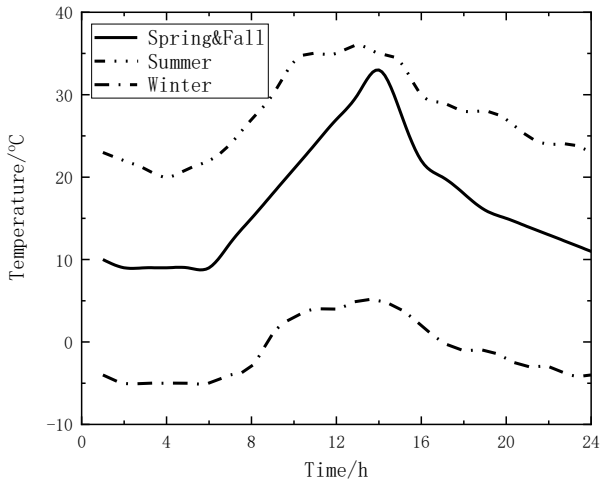

Figure 4-5 Typical temperature variations during spring, autumn, summer, and winter

In formula (2-1), it is evident that the metabolic rate of the user population has a significant impact on user thermal comfort. In reality, the user's condition determines the metabolic rate of the user population. Generally, the magnitudes of the user population's metabolic rate are as shown in the following Table 4-2:

Table 4-2 Magnitude of energy metabolism rate under different behaviors

behavior	M(W/m^2)
sleeping	46
sitting	70
shopping	93
working	170
walking	200

In daily life, most residents are usually awake from 8 AM to 10 PM. It can be approximated that the majority of people are in a sedentary state at home during this time, resulting in a metabolic rate of 70 W/m². From 11 PM to 7 AM, they are in a sleeping state, with a metabolic rate of 46 W/m². For commercial areas and industrial zones, their working hours correspond to shopping (93 W/m²) and working (170 W/m²) states, respectively.

4.2 Result and analysis

Due to varying temperature conditions in different seasons, the required heating and cooling loads to achieve optimal thermal comfort for users can differ significantly. Consequently, this leads to substantial disparities in the electrical, thermal, and cooling energy balances within the system. Therefore, this paper considers scheduling outcomes for three seasonal scenarios and conducts an analysis accordingly.

4.2.1 Result in transition seasons

For the integrated energy system, based on the electrical energy balance equation (2-38), it can be observed that the devices primarily associated with electrical energy balance include the micro gas turbine, energy storage battery, and external electricity purchase. The power outputs and actual electricity supply from these devices are illustrated in the following Figure 4-6.

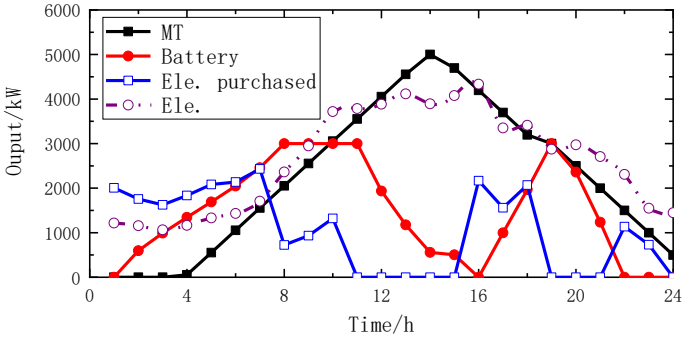

Figure 4-6 Electricity balance-related equipment output and power supply

Taking into account the external electricity purchase prices shown in Figure 4-2, during the off-peak hours from 1 AM to 7 AM when the prices are lower, the system heavily relies on purchasing electricity from the external grid due to its affordability. Concurrently, there is significant wind power output available. As only the electricity demand of residential users needs to be met during this time, the micro gas turbine doesn't need to generate power from 1 AM to 4 AM. The system's electricity supply is primarily fulfilled through a combination of external electricity purchase and wind power generation.

It's noteworthy that the energy storage battery's capacity gradually increases during this period, indicating that surplus energy is being stored. This excess energy is stored in the battery to prepare for higher demand periods, which are expected during peak hours.

From 8 AM to 5 PM, both commercial and industrial users have high electricity demands, leading to a peak in the system's external electricity supply during this time frame. Although the photovoltaic units contribute some electricity, there is still a substantial supply gap. Given the high cost of purchasing electricity from the external grid at this time, the micro gas turbine is the primary power generation source. As seen in the graph, the output of the micro gas turbine gradually increases after 8 AM, peaking around 3 PM and then gradually declining.

Simultaneously, the energy storage battery's capacity starts decreasing rapidly around 10 AM, as it's being utilized to meet the high demand. This decline continues until around 4 PM when the battery is nearly depleted. Between 4 PM and 5 PM, there's a dip in the external electricity purchase price, leading to a significant increase in external electricity purchasing during this period. This action helps alleviate the pressure on the micro gas turbine for power generation, allowing the battery to rapidly recharge in preparation for the next demand peak.

From 5 PM to 9 PM, the industrial users no longer require electricity. Although commercial and residential users are still in their electricity consumption peak, the energy storage battery has accumulated a significant amount of energy between 4 PM and 5 PM. Consequently, the micro gas turbine can reduce its power generation output during this period.

After 9 PM, the electricity demand from commercial users reaches its lowest point, and residential users also significantly reduce their electricity consumption.

Additionally, the external electricity purchase price is relatively low during this period. As a result, the micro gas turbine can operate at a lower output to meet the overall system demand.

According to the thermal energy balance equation (Equation 2-39), the devices related to thermal energy balance mainly consist of waste heat boilers, electric heat pumps, and thermal storage tanks. The output and actual heat supply of these devices are shown in Figure 4-7.

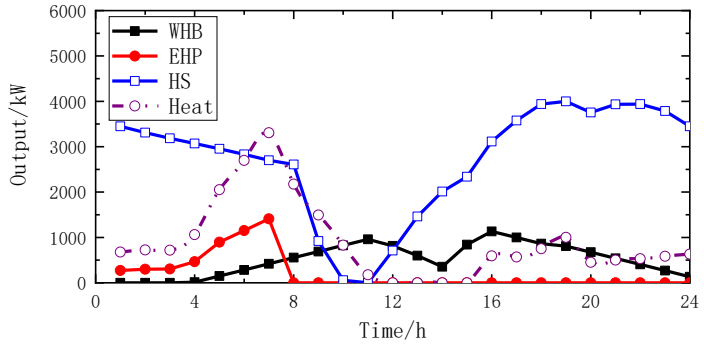

Figure 4-7 Heat balance-related equipment output and heating capacity

The main reason for heating is that the external temperature is lower than the comfort temperature. As indicated in Figure 4-5, during the typical spring and autumn seasons, the period from 12:00 PM to 4:00 PM is above the comfort temperature, while the rest of the time the temperature is below the comfort level. Larger temperature differences lead to greater heating demand. However, due to the fact that commercial and industrial users are not operational during the colder period from 4:00 AM to 8:00 AM, the system only needs to ensure heating for residential users. During the heating peak from 4:00 AM to 8:00 AM, the gas turbine is operating at a lower level, resulting in insufficient heat supply from the waste heat boiler. Therefore, the electric heat pump is used to provide heating. At the same time, the thermal storage tank absorbs heat from the waste heat boiler during the daytime and gradually releases it, continuing until around 9:00 AM when the stored heat reaches zero.

Based on the cooling energy balance formula (2-40), the devices related to cooling energy balance mainly consist of the absorption chiller and the electric refrigeration machine. The output and actual cooling capacity of these devices are shown in Figure 4-8.

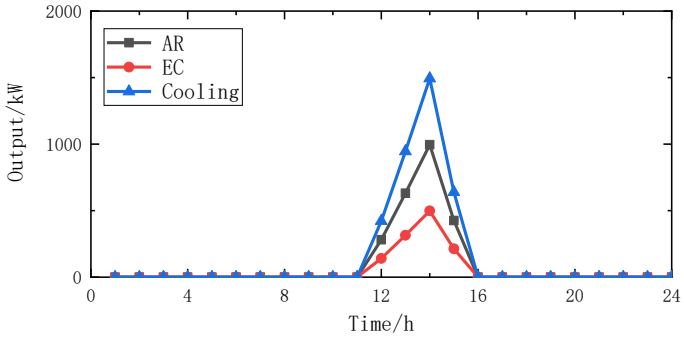

Figure 4-8 Cooling equipment output and cooling capacity related to cold balance

As indicated in Figure 4-5, during typical spring and autumn seasons, only from 12 to 16 hours is the outside temperature higher than the comfort temperature. Due to the elevated energy metabolism rates of both commercial and industrial users during this period (as shown in Table 4-2), a substantial amount of cooling energy is required. It's worth noting that the gas turbine is operating at a high level during this time, providing excess heat that can be used by the absorption chiller for cooling. Additionally, a certain amount of cooling can be achieved by the electric refrigeration machine, ensuring an adequate supply of cooling energy.

The results of the actual scheduling effects on indoor temperatures and thermal comfort for different user groups are shown in Figure 4-9.

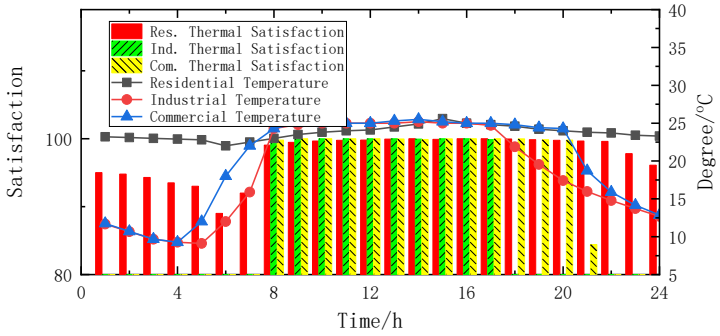

Figure 4-9 Satisfaction of thermal comfort and indoor temperature for each user

According to Table 4-2, it can be observed that from 8 AM to 4 PM, due to the higher energy metabolism rates of various user groups, even a small difference between indoor temperature and comfort temperature can lead to a significant decrease in thermal comfort. Therefore, during this period, the integrated energy system scheduling should ensure high thermal comfort for all three user groups. After 4 PM, it is still important to maintain high thermal comfort for both commercial and residential users. Subsequently, as commercial users cease operations, the system gradually reduces heating. Since residential users have lower energy metabolism rates

during the night, even if the indoor temperature is lower, their thermal comfort will not decrease significantly, remaining above 90. As a result, the system can significantly reduce its costs and energy consumption while only slightly decreasing its revenue.

The electricity satisfaction results for residential users, industrial users, and commercial users are presented in Figure 4-10 below.

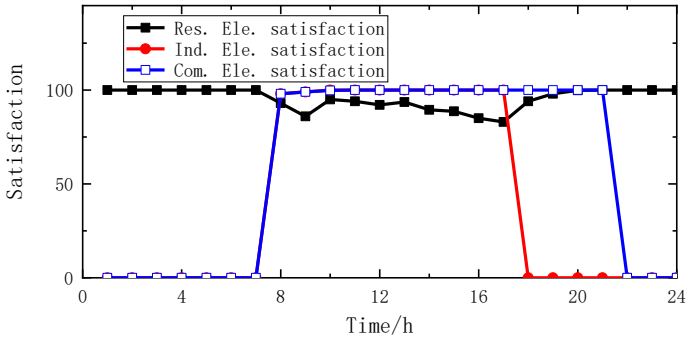

Figure 4-10 Satisfaction of electricity usage for each user

Due to the substantial power demand of industrial and commercial users during their daytime operations, and considering the inherent up and down constraints of the gas turbine (as specified in Equation (2-18)), the rapid increase in gas turbine power generation is limited. This leads to the necessity of reducing the electricity consumption of residential users from 8 AM onwards to ensure satisfactory power supply for industrial and commercial users. Between 8 AM and 6 PM, the electricity satisfaction for residential users experiences fluctuations and decreases. Starting from 6 PM, as the power demand from industrial users decreases, both residential and commercial users' electricity satisfaction can be maintained. From 9 PM to 7 AM the next day, since commercial operations are halted, the electricity satisfaction for residential users remains at a level of 100.

4.2.2 Result in summer

For the integrated energy system, according to the electrical energy balance equation (Equation 2-38), the devices related to electrical energy balance mainly include the micro gas turbine, energy storage battery, and external electricity purchase. The power output and actual supply of these devices are depicted in the following Figure 4-11.

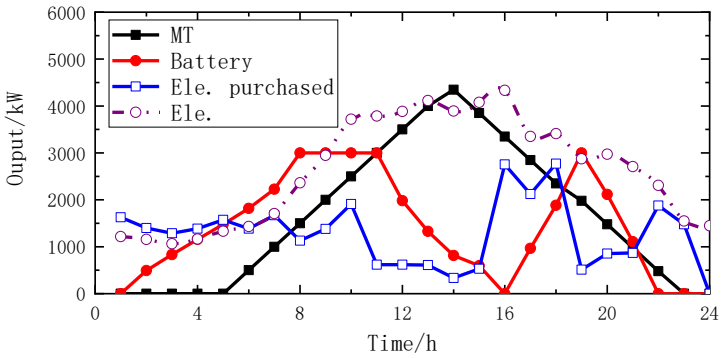

Figure 4-11 Electricity-related equipment output and power supply for electrical balance

The electricity purchasing behavior is similar to what was discussed in Section 4.2.1. During the low-priced period from 1 AM to 7 AM, the system purchases a significant amount of electricity from external sources due to the cheaper cost. However, unlike in Section 4.2.1, there is a substantial demand for cooling in the summer season after 7 AM. The absorption chiller alone might not be able to meet the extensive cooling demand, leading to the use of the electric chiller to provide additional cooling. As a result, the electricity demand is higher compared to the scenario in Section 4.2.1. This increased demand leads to significant energy storage in the energy storage battery. Additionally, during this period, wind power output is high and only the electricity demand of residential users needs to be met, allowing the micro gas turbine to remain idle between 1 AM and 4 AM while the system relies on the output of external electricity purchases and the wind power system to meet the demand.

From 8 AM to 5 PM, apart from the elevated electricity demand of commercial and industrial users mentioned in Section 4.2.1, the system faces substantial cooling demand during the daytime of summer. To ensure an adequate cooling capacity of the electric chiller, there is still a significant shortfall in supply, leading to the necessity of high-priced external electricity purchases during this period. Similarly to the previous scenario, the output of the micro gas turbine gradually increases after 8 AM, reaching its peak around 3 PM and then gradually decreasing after 3 PM. Simultaneously, the energy storage battery's capacity starts decreasing rapidly after 10 AM to accommodate the upcoming electricity demand peak, until it is nearly depleted by around 4 PM. Due to the appearance of a low pricing period for external electricity purchases between 4 PM and 5 PM, there is a substantial inflow of external electricity purchases during this time, alleviating the pressure on the micro gas turbine and allowing the energy storage battery to replenish its charge quickly.

From 5 PM to 9 PM, as industrial users no longer require electricity and considering

the gradual decrease in temperature observed in Figure 4-5, the cooling demand significantly decreases. Even though commercial and residential users are in a period of high electricity demand during this time, the energy storage battery has accumulated a substantial amount of energy from 4 PM to 5 PM. This allows the micro gas turbine to reduce its power output during this period. After 9 PM, as the electricity demand of commercial users reaches its lowest point and residential users greatly reduce their electricity consumption, the cost of external electricity purchases also becomes relatively low. Consequently, the micro gas turbine can maintain a low-level operation to meet the overall system demand until it stops functioning at 11 PM.

According to the thermal energy balance equation (2-39), the devices related to thermal energy balance mainly include waste heat boilers, electric heat pumps, and heat storage tanks. The output and actual heating capacity of these devices are shown in Figure 4-12.

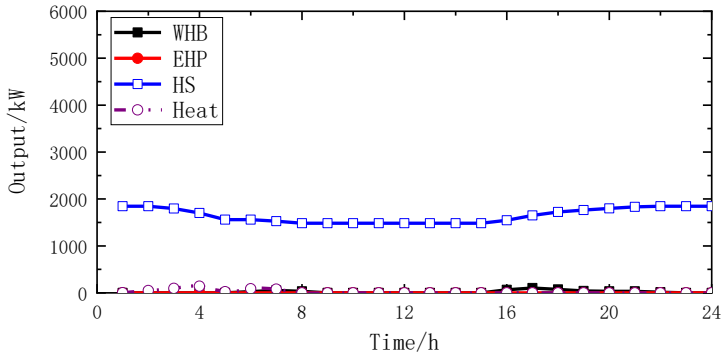

Figure 4-12 Heat-related equipment output and heating capacity for thermal balance

As indicated in Figure 4-5, during typical summer conditions, temperatures are below the comfort range from midnight to before 7 AM. Therefore, a certain amount of heating is still required to ensure user comfort. The waste heat boiler absorbs excess heat during the peak period of the gas micro-turbine operation and stores it in the heat storage tank. When temperatures are below the comfort range, the heat storage tank releases heat, ensuring an adequate supply of heating.

As per the cold energy balance formula (2-40), the devices related to cold energy balance primarily consist of the absorption chiller and electric chiller. The output and actual cooling capacity of these devices are shown in Figure 4-13.

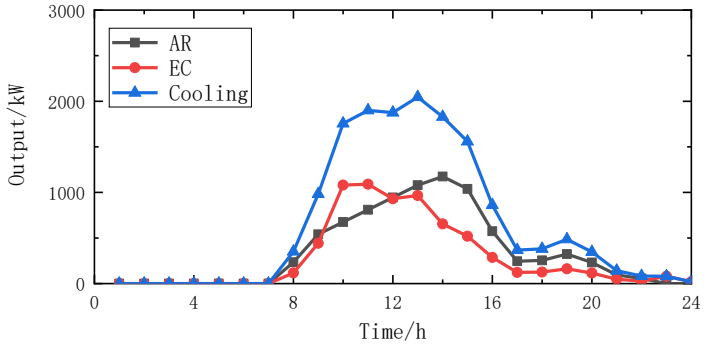

Figure 4-13 Cooling-related equipment output and cooling capacity for thermal balance

As indicated in Figure 4-5, during a typical summer season, from 7 AM until the early hours of the night, the external temperature remains higher than the comfortable temperature range. This is especially prominent around noon, at approximately 12 PM, when the temperature significantly exceeds the comfortable level. Additionally, during this time, residential, industrial, and commercial users are in an active state with higher energy metabolism rates, resulting in substantial cooling demand.

Previously, due to the time required for the output of the gas turbine to increase, the cooling demand was predominantly met by the electric chiller. However, when the gas turbine's output remained at a higher level, the output of the absorption chiller could also be maintained at a higher level. During this period, the cooling demand could be met by the more economical and environmentally friendly absorption chiller. As industrial and commercial users gradually concluded their activities, the cooling demand decreased, leading to a reduction in the outputs of both the electric chiller and the absorption chiller. When the gas turbine ceased to operate, coincidentally, there was no longer a need for cooling. Consequently, the absorption chiller and the electric chiller also ceased operation.

The actual scheduling results for indoor temperatures and thermal comfort satisfaction of different user groups are presented in Figure 4-14.

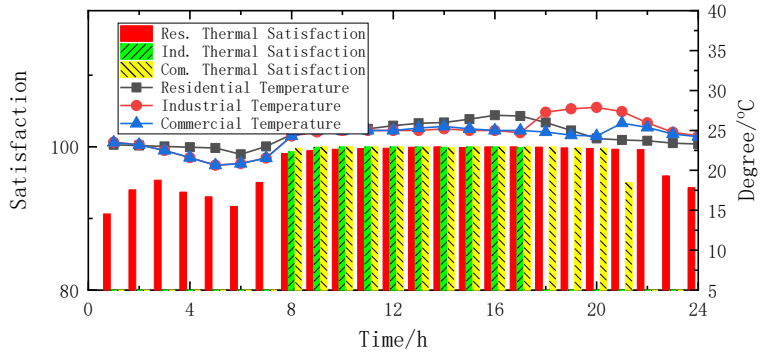

Figure 4-14 Thermal satisfaction of each user in relation to indoor temperature

Similar to the situation described in 4.2.1, from 22:00 to 7:00, as both industrial and commercial users do not require temperature adjustments and residential users have a lower metabolic rate during sleep, only a small amount of heating is necessary to ensure thermal comfort within an acceptable range. During this period, the system relies mainly on the heat stored in the thermal storage tank, which is derived from the waste heat boiler. This source of heat incurs minimal cost, allowing for a reasonable balance between user thermal satisfaction and energy expenses.

Similarly, based on Table 4-2, between 8:00 and 16:00, the high metabolic rates of the user groups combined with the high outdoor temperatures in summer necessitate significant energy consumption for cooling to maintain their thermal comfort at 100%. Consequently, the system has to purchase external electricity at a higher cost to maintain its cooling capacity. As the industrial users approach the end of their work hours and the outdoor temperature stabilizes, the output of the gas turbine can be lowered. By 22:00, the gas turbine is ready to stop working, resulting in a slight decrease in thermal comfort satisfaction for commercial users, although still within an acceptable range. As temperatures continue to drop below the comfort level, commercial users close their businesses, and the system only needs to consider the thermal satisfaction of residential users.

The user satisfaction results for residential, industrial, and commercial users' electricity usage are depicted in Figure 4-15.

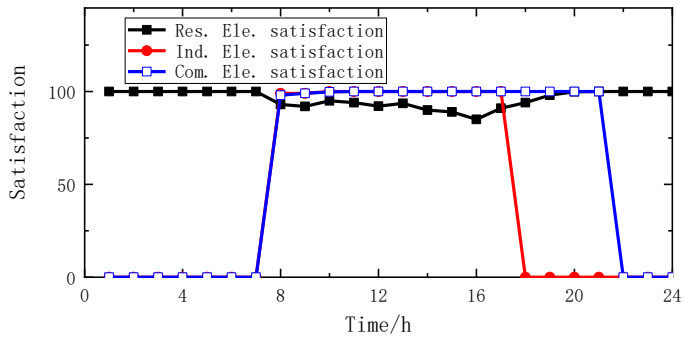

Figure 4-15 Satisfaction of electricity usage for each user

The electricity satisfaction results are similar to those in typical spring and autumn scenarios described in 4.2.1, but there are differences. After 7:00, the rapid temperature changes caused by industrial and commercial users result in significant cooling demand, leading to a larger reduction in residential electricity usage compared to the situation shown in Figure 4-10 of 4.2.1. Between 8:00 and 18:00, residential electricity satisfaction experiences fluctuating declines. Starting from 18:00, with the cessation

of industrial user electricity demand, both residential and commercial electricity satisfaction can be adequately met. Similarly, from 21:00 to 7:00 of the following day, as commercial users close their businesses, the residential electricity demand is fully satisfied.

4.2.3 Result in winter

The electricity balance formula (2-38) indicates that for the integrated energy system, the devices primarily responsible for electricity balance are the micro gas turbine, energy storage battery, and external electricity purchase. The output and actual electricity supply from these devices are depicted in Figure 4-16.

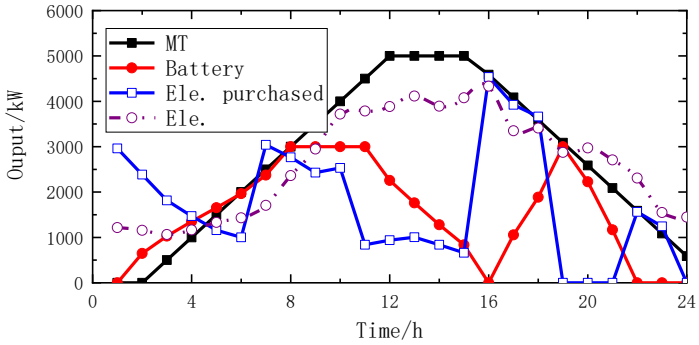

Figure 4-16 Electricity balance-related device output and electricity generation

Unlike the typical spring and autumn scenarios in Section 4.2.1 and the typical summer scenario in Section 4.2.2, in the typical winter scenario, the micro gas turbine operates at its maximum power output for the longest duration. This is primarily due to the fact that during typical winter, all user types - residential, commercial, and industrial - experience high energy metabolism rates, and the outdoor temperature is significantly low, leading to substantial heating demands. Combined with electricity demands during this time, the gas turbine must operate at high power levels for an extended period to ensure sufficient power supply, preheating demands for the waste heat boiler, and heating requirements for the electric heat pump.

Similarly, external electricity purchases are significantly higher than those in the typical spring and autumn scenarios as well as the typical summer scenario. Not only does external electricity purchasing exceed those from the previous two seasons during the low-price periods, but it also surpasses them during peak-price periods. Specifically, from 1 AM to 7 AM, due to low electricity prices, the gas turbine operates at a lower output level to save costs, and heating demands are met through the electric heat pump, necessitating a large amount of electricity purchase from the external grid to fulfill the system's needs. During the high-price period from 7 AM to 3 PM, the system is forced to purchase electricity at high prices until the gas turbine gradually ramps up to high

output levels, at which point external electricity purchases drop to a relatively low level of around 1000 kW. However, from 3 PM onwards, in order for the gas turbine to operate at low output levels during the night, a substantial amount of electricity is purchased from the external grid. This purchased electricity is stored in the energy storage battery, which is already depleted by 4 PM to ensure nighttime power supply.

For the energy storage battery, it mainly accumulates low-cost purchased external electricity before 8 AM, maintaining a fully charged state between 8 AM and 12 PM when the battery is at its capacity. After 11 AM, when electricity prices increase, external electricity purchases reduce in scale, causing the energy storage battery to discharge its stored energy into the system. This continues until the battery is completely depleted by 4 PM.

The devices related to thermal energy balance, as indicated by the thermal energy balance formula (2-39), primarily consist of the waste heat boiler, electric heat pump, and thermal energy storage tank. The output and actual heat supply from these devices are illustrated in Figure 4-17.

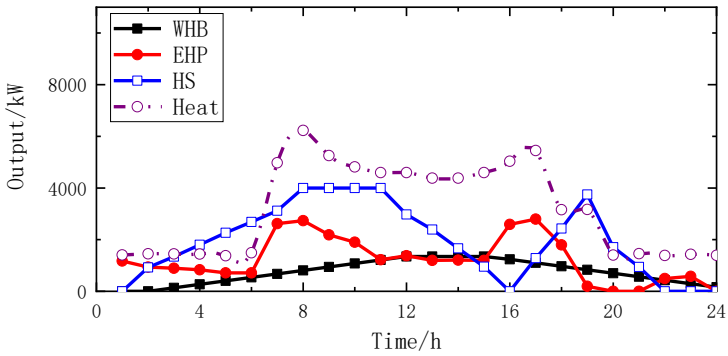

Figure 4-17 Heat balance-related device output and heating capacity

In the typical winter scenario, the outdoor temperature remains below the comfort temperature throughout the 24-hour period, requiring the system to provide heating continuously. As mentioned in Section 4.2.1, the larger the difference between outdoor temperature and comfort temperature, the greater the heating demand. Therefore, winter is a period with exceptionally high heating requirements. In Figure 4-17, the heating demand can be roughly divided into three levels.

The highest heating demand occurs around 7 AM to 5 PM, during which time all user types - residential, commercial, and industrial - require heating. This results in the overall heating demand being at its peak during this period. The presence of a higher heating demand at the beginning and end of this high demand period is due to commercial and industrial users cooling down overnight, resulting in lower indoor

temperatures. Consequently, heating demands are intensified during the early hours. Similarly, the elevated heating demand around 4 PM is due to the end of the daytime and the subsequent temperature drop, increasing the heating demands of all user types.

After 5 PM, as industrial users conclude their heating demands, the overall heating pressure is significantly reduced as only commercial and residential users' heating needs need to be addressed. Post 9 PM, with the gradual reduction in heating demand from commercial users, the heating demand reaches its lowest level.

In terms of the primary heating equipment, the waste heat boiler generally follows the output curve of the micro gas turbine as depicted in Figure 4-16. All the waste heat generated by the gas turbine is utilized for heating, leading to a high output of the electric heat pump during the periods when the gas turbine's output is low, but the heating demand is high (around 7 AM to 9 AM and around 4 PM). The thermal energy storage tank stores heat until around 12 PM and then releases it as the gas turbine's power output decreases. It absorbs heat around 4 PM and releases it during the night, helping alleviate the heating gap and allowing the gas turbine to operate at low output levels.

The devices related to cold energy balance, as indicated by the cold energy balance formula (2-40), mainly consist of the absorption chiller and the electric chiller. The output and actual cooling supply from these devices are illustrated in Figure 4-18.

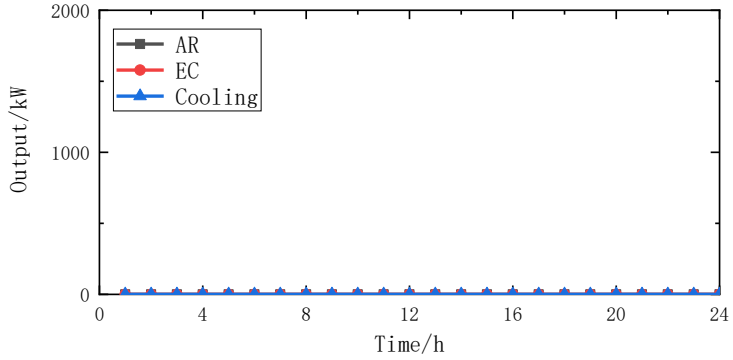

Figure 4-18 Cooling balance-related device output and cooling capacity

In typical winter conditions, cooling is not required, so the equipment related to the cooling energy balance remains inactive.

The actual scheduling effects on indoor temperatures and thermal comfort levels for different user groups are shown in Figure 4-19.

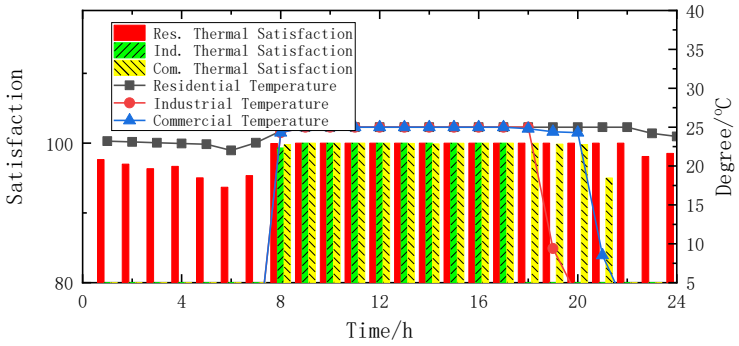

Figure 4-19 Thermal satisfaction of each user with indoor temperature

Similar to the analysis for typical spring and autumn seasons in section 4.2.1, during the night in typical winter conditions, the energy metabolism rate of residents is lower due to their sleep state. As a result, the system can reduce the heating supply for temperature adjustment. In typical winter scenarios, the energy management of the integrated energy system decreases the heating demand for residential users during the night. This reduction is achieved while ensuring a high level of thermal comfort for residents, thereby lowering the operational costs of the system. From 8 AM to 8 PM, given that the gas turbine is already operating at a higher level, the system can ensure a satisfactory level of heating comfort for residential, industrial, and commercial users.

The satisfaction levels of electricity usage for residential, industrial, and commercial users are shown in Figure 4-20.

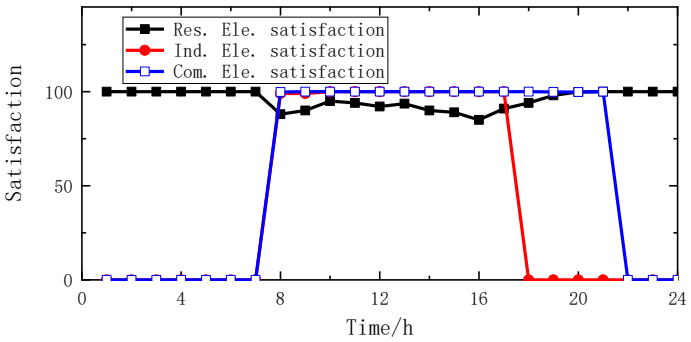

Figure 4-20 Electricity satisfaction for each user

The trend in the graph is similar to the typical spring and autumn scenarios in section 4.2.1, as well as the typical summer scenario in section 4.2.2. However, in the case of 7 AM, the system starts heating, and industrial and commercial users must ensure that their heating demands are fully met when initiating heating. This necessity leads to a greater reduction in the thermal comfort of residential users between 7 AM and 8 AM. Combining this with the high points in heating demand seen in Figure 4-17 at 8 AM and 5 PM, it becomes apparent that there are significant energy pressures on the system, resulting in a reduction in user electricity consumption around these timeframes to ensure the overall economic efficiency of the system.

4.2.4 Dispatch analysis

Table 4-3 Economic results without elastic load scheduling

	Spring and Autumn	summer	winter
Operating cost (yuan)	61205.38	57618.96	90812.91
Residential cooling cost (yuan)	470.49	2163.2	0.00
Industrial cooling cost(yuan)	879.32	3509.04	0.00
Commercial cooling cost (yuan)	636.48	3051.36	0.00
Residential heating cost (yuan)	5504.24	276.46	18352.36
Industrial heating cost (yuan)	3145.95	0.00	12423.21
Commercial heating cost (yuan)	3834.35	0.00	13502.06
Residential electricity cost (yuan)	15508.62	15508.62	15508.62
Industrial electricity cost (yuan)	11564.09	11564.09	11564.09
Commercial electricity cost (yuan)	20043.92	20043.92	20043.92
Cooling cost (yuan)	1986.29	8723.60	0.00
Heating cost (yuan)	12484.51	276.46	44277.64
Electricity cost (yuan)	47116.63	47116.63	47116.63
Total cost (yuan)	61587.44	56116.71	91394.27
Net income (yuan)	382.06	-1502.26	581.36

Based on the scenario data provided in section 4.1, Table 4-3 shows the comprehensive energy scheduling results without flexible load dispatch. In this scheduling, calculations are performed solely based on user energy demands. On the other hand, Table 4-4 presents the economic results obtained after implementing flexible load dispatch for the same case and scenario.

Table 4-4
Economic results of elastic load scheduling

	Spring and Autumn	summer	winter
Operating cost (yuan)	51433.08	51034.08	72051.99
Residential cooling cost (yuan)	380.01	1747.22	0.00
Industrial cooling cost(yuan)	879.32	3509.04	0.00
Commercial cooling cost (yuan)	624.24	2992.68	0.00
Residential heating cost (yuan)	3321.51	166.83	10758.28
Industrial heating cost (yuan)	2332.34	0.00	8996.12
Commercial heating cost (yuan)	2776.61	0.00	9777.35
Residential electricity cost (yuan)	11993.33	11993.33	11993.33
Industrial electricity cost (yuan)	11564.08	11564.08	11564.08
Commercial electricity cost (yuan)	19509.41	19509.41	19509.41
Cooling cost (yuan)	1883.57	8248.92	0.00
Heating cost (yuan)	8430.45	166.83	29848.17
Electricity cost (yuan)	43066.83	43066.83	43066.83
Total cost (yuan)	53380.86	51482.59	72915.01
Net income (yuan)	1947.77	448.51	863.02

The comparison between Table 4-4 and Table 4-3 clearly indicates that after implementing flexible load dispatch, the overall system operating costs have significantly decreased across all three seasonal scenarios. In the typical spring and autumn scenarios, the total scheduling costs have reduced by 15.97% and 11.42% respectively, while in the typical summer scenario, the reduction is 20.65%. For

residential users, the total energy costs have decreased by 13.32% in spring and autumn, 8.25% in summer, and 20.21% in winter. The greatest reductions are observed in summer, followed by spring and autumn.

Looking more closely, during spring and autumn, the costs associated with cooling decrease by approximately 15% due to flexible load dispatch. This reduction is attributed to adjustments in the pricing structure for cooling services. By employing game theory in flexible load dispatch, the comprehensive energy system service provider partially passes on cost savings, leading to a decrease in cooling costs. For heating costs, the reduction is more substantial, particularly during the night when flexible load dispatch for residential users allows for overall system cost savings. Compared to the approximately 20% reduction for industrial and commercial users, the reduction for residential users is as high as 39.65%. The service provider reallocates the cost savings from flexible load dispatch, providing the largest relief to the most affected residential users and to some extent to the commercial and industrial users. The reduction in electricity costs is relatively minor, mainly due to the absence of strong temporal and spatial variations in electricity demand satisfaction.

In summer, the reduction in cooling costs is similar to that in spring and autumn, primarily occurring when residential users are asleep and the cooling demand is low. For heating, a small amount is provided, relying on waste heat and thermal storage. In terms of electricity supply, due to limitations in significant adjustments for cooling loads, the cost savings are not as extensive as in spring and autumn. Overall, summer experiences the lowest degree of reduction from flexible load dispatch, resulting in a comparatively modest decrease in system costs and user expenses.

In winter, with no cooling demand, the primary energy requirement is for heating. Notably, during the daytime, the overlap of heating and electricity consumption peaks prompts a slight reduction in residential heating, mitigating the high operating costs associated with heating peaks. Additionally, during the colder nights when residential heating is highly required, flexible load dispatch helps in substantial cost savings. This is reflected in the results, where the reduction in heating costs for residential users exceeds 40%, while industrial and commercial users experience reductions of around 20%.

In summary, flexible load dispatch alleviates the rise in system costs during peak periods and optimizes the allocation of energy during times of varying user demand intensity (utility function parameters). This approach enhances user utility while

reducing a certain amount of load, thereby optimizing system operating costs and ensuring that users also benefit from the cost savings achieved through game theory-based approaches.

4.3 Sensitivity analysis

The expression of thermal comfort using equations (2-6) to (2-9) reveals a significant impact of the metabolic rate (M). The thermal comfort satisfaction under different metabolic rates and various room temperatures is illustrated in Figure 4-21. The graph clearly shows that as the metabolic rate increases, the rate of decrease in satisfaction when deviating from the comfort temperature is also higher. Particularly when the metabolic rate M equals 170, the satisfaction level drops to 0 when the temperature exceeds 33 degrees or falls below 14 degrees. Considering the user utility function in equation (2-15), users are unwilling to pay for heating or cooling at such temperatures.

Furthermore, it's important to note that for larger metabolic rates M, the rate of decrease in satisfaction is faster for higher temperatures compared to lower temperatures. This observation aligns with common understanding and experiences in real life.

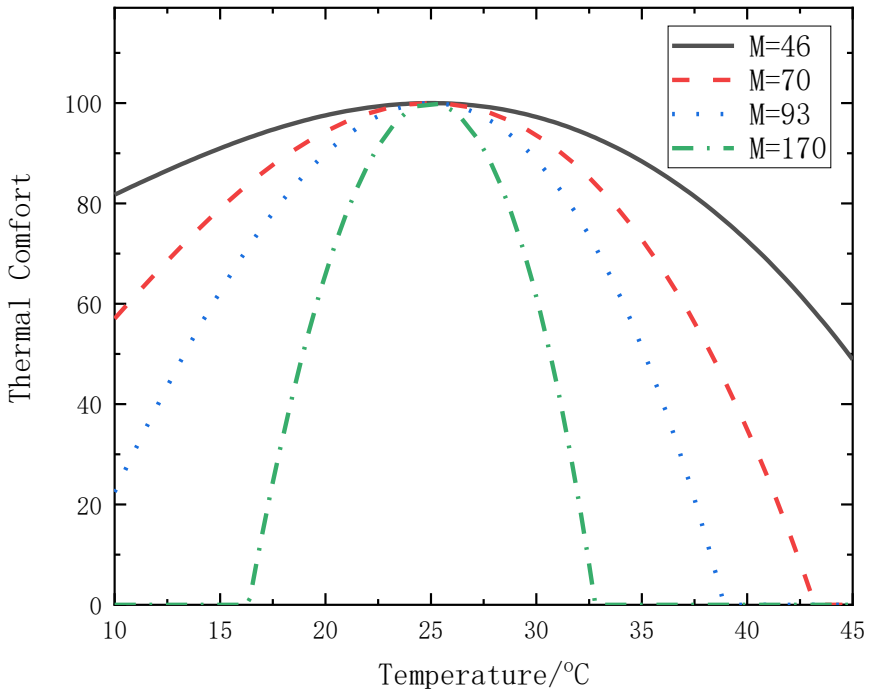

Figure 4-21 Thermal satisfaction at different temperatures for various energy metabolism rates (M)

The metabolic rate (M) has a significant impact on actual thermal comfort satisfaction,

and changing user behavior can indeed lead to changes in the metabolic rate. For instance, in the scenario described in Section 4.1, where industrial users are active from 8 AM to 5 PM, let's assume that these users take a lunch break during which they are mostly sedentary. If we consider the lunch break to be from 12 PM to 1 PM and incorporate this into the scheduling, the results are presented in Figure 4-22. To provide a more detailed insight into the changes in scheduling outcomes, Figure 4-22 primarily illustrates the indoor temperature and thermal comfort satisfaction during the summer hours of 9 AM to 3 PM, where the effects are most pronounced.

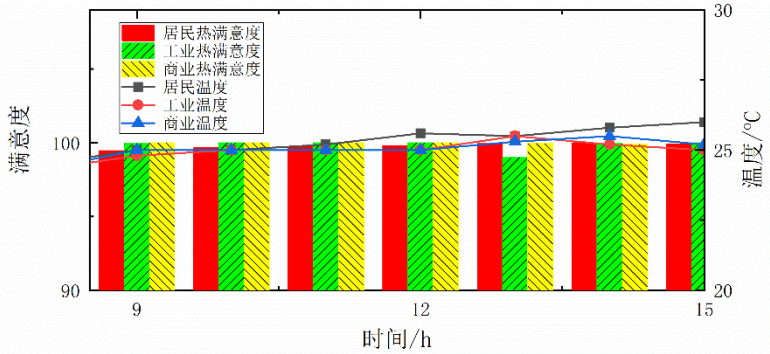

Figure 4-22 Indoor temperature and thermal satisfaction with midday rest

For better comparison, the indoor temperature and thermal comfort satisfaction data from Figure 4-14 during the hours of 9 AM to 3 PM have been extracted and are presented in Figure 4-23. Upon comparison, it is evident that with the implementation of the lunch break, particularly during the peak cooling demand hours in summer, the main source of flexibility before the inclusion of the industrial user's lunch break is the relatively less sensitive residential users. This is reflected in Figure 4-23, where a slightly higher indoor temperature for residential users can be observed.

After incorporating the lunch break for the industrial user, both residential and industrial users have some degree of flexibility. In Figure 4-22, one can observe that both user groups experience a certain increase in temperature. However, since the industrial user's metabolic rate returns to normal after 1 PM, their temperature returns to the comfort zone. Consequently, residential users bear a larger portion of the flexibility, resulting in a higher temperature increase as indicated in the figure.

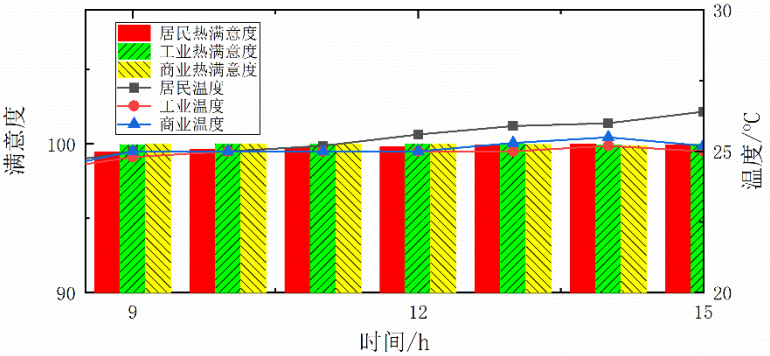

Figure 4-23 Indoor temperature and thermal satisfaction without midday rest

4.4 本章小结

In Chapter 4, the simulation configuration data was introduced in Section 4.1, encompassing the rated capacities and economic parameters of the system's devices, user states, seasonal scenario data, and the output predictions of the distributed generation system. Subsequently, in Section 4.2, an analysis of the scheduling results for different seasonal scenarios was conducted. These results primarily include the output and energy supply status of the integrated energy system's devices, indoor temperature and thermal comfort satisfaction for users, and user satisfaction with electricity consumption. An economic analysis was then carried out on these results.

The findings indicate that flexible load scheduling effectively taps into the energy consumption flexibility of users, thus reducing the overall operational costs of the system. This is achieved by distributing the saved cost benefits to both users and the integrated energy system through a game-theoretical approach. Lastly, in Section 4.3, a sensitivity analysis was performed to assess the impact of changes in energy metabolism rates and user states on the scheduling results.

5 Conclusion

This paper introduces a comprehensive energy flexible load scheduling method based on master-slave game theory. This method addresses the flexible scheduling challenges in integrated energy systems by establishing user-centric energy satisfaction and utility models, describing the utility of users' energy experiences, and considering the impact of user payment limits on energy satisfaction. Building upon this foundation and the established integrated energy system operation model, the paper presents a master-slave game-based flexible load scheduling approach. This approach employs a hierarchical game structure to achieve practical flexible load scheduling, striking a balance between user energy experience and the optimal operation of the integrated energy system. The game equilibrium is then solved using the Genetic Algorithm (GBO). Through case studies, the results demonstrate that the proposed game-based flexible load scheduling for integrated energy users effectively reduces energy costs for both the integrated energy system and users. This confirms the efficacy of the proposed scheduling method.

5.1 Conclusion

Summarizing the research of this paper, the main achievements are as follows:

1、Innovatively established a model for user energy satisfaction and utility function to describe the satisfaction experienced by users in integrated energy heating, cooling, or power supply scenarios. This model also takes into account the impact of user energy expenses on their energy experience, thus effectively describing users' experiences with energy consumption in integrated energy supply scenarios. The establishment of this model lays the foundation for exploring user energy flexibility in subsequent elasticity scheduling models.

2、Proposed a flexible load scheduling method based on master-slave game. This method achieves cost reduction in integrated energy system scheduling by applying flexible load scheduling based on the principle of maximizing user energy utility functions in practical integrated energy scheduling. The method then employs hierarchical game theory to allocate the reduced economic cost effectively, achieving a win-win situation for both users and the integrated energy system.

3、Furthermore, the introduced game-based integrated energy user flexible load scheduling approach in this study demonstrates notable cost reduction and user fee reduction effects. The extent of cost reduction and user fee reduction varies significantly under different seasonal temperature conditions. Specifically, the largest

reduction occurs during winter, at around 30%, followed by spring and autumn at approximately 20%, while the least reduction is observed in summer, around 10%. The analysis results indicate that this variability is mainly due to the diverse distribution of user energy flexibility under different temperature conditions. This underscores the substantial economic benefits that can be achieved by tapping into the flexibility of energy consumption through flexible load scheduling, validating the effectiveness of the proposed approach in this study.

5.2 Future work

Building upon the aforementioned work, further in-depth research is needed in the following areas:

1、The assumption made in this study about the distribution of energy metabolism rates is somewhat idealized. As revealed by the sensitivity analysis in Section 4.3, variations in energy metabolism rates, or rather the users' own states, directly reflect the spatial and temporal distribution of their heat demand levels. It's precisely due to this non-uniformity in the spatial and temporal distribution that the flexibility of energy consumption differs across different time periods. To better tap into this flexibility, a more accurate assessment of user energy states is required. The user state assessment provided in Section 4.1, as a simplification of real-life conditions, will likely be more complex in actual situations. This presents both a challenge and an opportunity for further exploration of flexibility.

2、The scheduling research conducted in this paper only covers a few typical weather scenarios. In reality, with a sufficient amount of weather data, it's entirely possible to conduct multi-year scheduling studies, thus comprehensively evaluating the effectiveness of the proposed methods. This approach would not only validate the effectiveness of the methods but also contribute to the advancement of theoretical research in practical integrated energy system scheduling.

3、The system configuration parameters presented in Section 4.1 were established before the actual scheduling validation, leaving room for optimization. Essentially, what is lacking is a comprehensive energy system planning based on the scheduling results. Building on the scheduling methods proposed in this paper and utilizing multi-year weather data, more effective integrated energy system planning research can be carried out, taking into account the real-world scheduling outcomes.

Reference

[1] Alex Q. Huang, Mariesa L. Crow, Gerald Thomas Heydt, et al. The Future Renewable Electric Energy Delivery and Management (FREEDM) System: The Energy Internet[J]. Proceedings of the IEEE,2011,99(1):133-143.

[2] Fanxin Kong, Chuanshen Dong, Xue Liu, et al. Quantity Versus Quality: Optimal Harvesting Wind Power for the Smart Grid[J]. Proceedings of the IEEE,2014,102(11): 1762-1776.

[3] J. Rifkin. The third industrial revolution: How lateral power is transforming energy, the economy and the world[M]. New York: Palgrave MacMillan,2011:5-20.

[4] 国家发展改革委员会，国家能源局，工业和信息化部. 关于推进“互联网++”智慧能源发展的指导意见，发改能源[2016]392[R]. 北京：国家发展改革委员会，国家能源局，工业和信息化部，2013.

[5] 余晓丹,徐宪东,陈硕翼,吴建中,贾宏杰.综合能源系统与能源互联网简述[J].电工技术学报,2016,31(01):1-13.

[6] Qingmei Wen, Gang Liu, Zhenghua Rao, et al. Applications, evaluations and supportive strategies of distributed energy systems: A review[J]. Energy & Buildings,2020,225:110314.

[7] Ivan Bačeković, Poul Alberg Østergaard. A smart energy system approach vs a non-integrated renewable energy system approach to designing a future energy system in Zagreb[J]. Energy,2018,155:824-837.

[8] Pierluigi Mancarella. MES (multi-energy systems): An overview of concepts and evaluation models[J]. Energy,2014,65:1-17.

[9] Wei Gu, Zhi Wu, Rui Bo, et al. Modeling, planning and optimal energy management of combined cooling, heating and power microgrid: A review[J]. International Journal of Electrical Power and Energy Systems,2014,54:26-37.

[10] Alberto Fichera, Mattia Frasca, Valentina Palermo, et al. Application of the Complex Network Theory in Urban Environments. A Case Study in Catania[J]. Energy Procedia,2016,101:345-351.

[11] Sayyed Faridoddin Afzali, Vladimir Mahalec. Novel performance curves to determine optimal operation of CCHP systems[J]. Applied Energy,2018,226:1009-1036.

[12] Jian Zhang, Heejin Cho, Pedro J. Mago, et al g. Multi-Objective Particle Swarm Optimization (MOPSO) for a Distributed Energy System Integrated with Energy Storage[J]. Journal of Thermal Science,2019,28(6):1221-1235.

[13] Hamed Ershadi, Arash Karimipour. Present a multi-criteria modeling and optimization (energy, economic and environmental) approach of industrial combined cooling heating and power (CCHP) generation systems using the genetic algorithm, case study: A tile factory[J]. Energy,2018,149:286-295.

[14] Pierluigi Mancarella, Gianfranco Chicco, Tomislav Capuder. Arbitrage opportunities for distributed multi-energy systems in providing power system ancillary services[J]. Energy,2018,161:381-395.

[15] Sayyed Faridoddin Afzali, Vladimir Mahalec. Optimal design, operation and analytical criteria for determining optimal operating modes of a CCHP with fired HRSG, boiler, electric chiller and absorption chiller[J]. Energy,2017,139:1052-1065.

[16] Longxi Li, Hailin Mu, Weijun Gao, et al. Optimization and analysis of CCHP system based on energy loads coupling of residential and office buildings[J]. Applied Energy,2014,136:206-216.

[17] Ligai Kang, Junhong Yang, Qingsong An, et al. Effects of load following operational strategy on CCHP system with an auxiliary ground source heat pump considering carbon tax and electricity feed in tariff[J]. Applied Energy,2016,194:454-466.

[18] Martin Geidl, Gaudenz Koeppel, Patrick Favre-Perrod, et al. Energy Hubs for the Future[J]. IEEE power & energy magazine,2007,5(1):24-30.

[19] Yi Wang, Ning Zhang, Chongqing Kang, et al. Standardized Matrix Modeling of Multiple Energy Systems.[J]. IEEE Trans. Smart Grid,2019,10(1):257-270.

[20] Morteza Nazari-Heris, Behnam Mohammadi-Ivatloo, Somayeh Asadi. Optimal operation of multi-carrier energy networks with gas, power, heating, and water energy sources considering different energy storage technologies[J]. Journal of Energy Storage,2020,31:101574.

[21] Wei Gu, Jun Wang, Shuai Lu, et al. Optimal operation for integrated energy system considering thermal inertia of district heating network and buildings[J]. Applied Energy,2017,199:81-89.

[22] Eduardo Alejandro Martinez-Cesena, Pierluigi Mancarella. Energy Systems Integration in Smart Districts: Robust Optimisation of Multi-Energy Flows in Integrated Electricity, Heat and Gas Networks.[J]. IEEE Trans. Smart Grid,2019,10(1):1122-1131.

[23] Morteza Nazari-Heris, Behnam Mohammadi-Ivatloo, Somayeh Asadi. Optimal Operation of Multi-Carrier Energy Networks Considering Uncertain Parameters and Thermal Energy Storage[J]. Sustainability,2020,12(12):5158.

[24] Samaneh Pazouki, Mahmoud-Reza Haghifam. Optimal planning and scheduling of energy hub in presence of wind, storage and demand response under

uncertainty[J]. International Journal of Electrical Power and Energy Systems,2016,80:219-239.

[25] Zhaoguang Pan, Qinglai Guo, Hongbin Sun. Interactions of district electricity and heating systems considering time-scale characteristics based on quasi-steady multi-energy flow[J]. Applied Energy,2016,167.

[26] L.X. Wang, J.H. Zheng, M.S. Li, et al. Multi-time scale dynamic analysis of integrated energy systems: An individual-based model[J]. Applied Energy,2019,237:230-243.

[27] Yizhou Zhou, Zhinong Wei, Guoqiang Sun, et al. A robust optimization approach for integrated community energy system in energy and ancillary service markets[J]. Energy,2018,148:1-15.

[28] Ma Li, Liu Nian, Zhang Jianhua, et al. Real-Time Rolling Horizon Energy Management for the Energy-Hub-Coordinated Prosumer Community From a Cooperative Perspective[J]. IEEE Transactions on Power Systems,2019,34(2): 1227-1242.

[29] Yifei Wang, Zhiheng Huang ,Zhenhao Li, et al. Transactive Energy Trading in Reconfigurable Multi-carrier Energy Systems[J]. Journal of Modern Power Systems and Clean Energy,2020,8(1):67-76.

[30] Jianxiao Wang, Haiwang Zhong, Ziming Ma, et al. Review and prospect of integrated demand response in the multi-energy system[J]. Applied Energy,2017,202:772-782.

[31] Liangce He, Zhigang Lu, Lijun Geng, et al. Environmental economic dispatch of integrated regional energy system considering integrated demand response[J]. International Journal of Electrical Power and Energy Systems,2020,116(C):105525.

[32] Rune Grønborg Junker, Carsten Skovmose Kallesøe, Jaume Palmer Real, et al. Stochastic nonlinear modelling and application of price-based energy flexibility[J]. Applied Energy,2020,275:105096.

[33] Joakim Widén, Ewa Wäckelgård. A high-resolution stochastic model of domestic activity patterns and electricity demand[J]. Applied Energy,2009,87(6):1880-1892.

[34] Toshinobu Shintai,Yushi Miura,Toshifumi Ise. Oscillation Damping of a Distributed Generator Using a Virtual Synchronous Generator[J]. IEEE Transactions on Power Delivery,2014,29(2):668-676.

[35] Henrik Lund,Ebbe Muenster. Integrated energy systems and local energy markets[J]. Energy policy,2006,34(10):1152-1160.

[36] Binod Prasad Koirala,Ellen van Oost, Henny van der Windt. Community energy storage: A responsible innovation towards a sustainable energy system?[J]. Applied Energy,2018,231:570-585.

[37] Robert Spangler, Raymond Shoults. Power Generation, Operation, and Control [J]. IEEE Power and Energy Magazine,2014,12(4):25-37.

[38] Laura-Lucia Richter, Michael G. Pollitt. Which smart electricity service contracts will consumers accept? The demand for compensation in a platform market[J]. Energy Economics,2018,72:436-450.

[39] Schäfer M,Hobus I, Schmitt T G. Energetic flexibility on wastewater treatment plants.[J]. Water science and technology: a journal of the International Association on Water Pollution Research,2017,76(5):1225-1233.

[40] P. Finn,C. Fitzpatrick, D. Connolly,M. Leahy, L. Relihan. Facilitation of renewable electricity using price based appliance control in Ireland's electricity market[J]. Energy,2011,36(5):1225-1233.

[41] Rami El Geneidy, Bianca Howard. Contracted energy flexibility characteristics of communities: Analysis of a control strategy for demand response[J]. Applied Energy,2020,263(C):114600.

[42] De Zotti Giulia, Pourmousavi S. Ali, Madsen Henrik, et al. Ancillary Services 4.0: A Top-to-Bottom Control-Based Approach for Solving Ancillary Services Problems in Smart Grids[J]. IEEE Access,2018,6: 11694-11706.

[43] Jimin Kim, Taehoon Hong, Jaemin Jeong, et al. An optimization model for selecting the optimal green systems by considering the thermal comfort and energy consumption[J]. Applied Energy,2016,169:682-695.

[44] Lizhen Wang, Donglin Zheng. Integrated analysis of energy, indoor environment, and occupant satisfaction in green buildings using real-time monitoring data and on-site investigation[J]. Building and Environment,2020,182:107014.

[45] Sabita Maharjan, Quanyan Zhu, Yan Zhang, et al. Dependable Demand Response Management in the Smart Grid: A Stackelberg Game Approach[J]. IEEE Trans. Smart Grid,2013,4(1):120-132.

[46] Maharjan Sabita, Zhu Quanyan, Zhang Yan, et al. Demand Response Management in the Smart Grid in a Large Population Regime[J]. IEEE transactions on smart grid,2016,7(1):189-199.

[47] Zhong Fan. A Distributed Demand Response Algorithm and Its Application to PHEV Charging in Smart Grids[J]. IEEE Trans. Smart Grid,2012,3(3):1280-1290.

[48] Fanger, P.O. Thermal comfort. Analysis and applications in environmental engineering[M]. Denmark: Danish Technical Press, 1970:14-29.

[49] Xu Xiao, Hu Weihao, Liu Wen, et al. Risk management strategy for a renewable power supply system in commercial buildings considering thermal comfort and stochastic electric vehicle behaviors[J]. Energy Conversion and Management,2021,230:113831.

[50] Sally Shahzad, John Brennan, Dimitris Theodossopoulos, et al. Energy and comfort in contemporary open plan and traditional personal offices[J]. Applied Energy,2016,185:1542-1555.

[51] A.S.O. Ogunjuyigbe,T.R. Ayodele ,O.A. Akinola. User satisfaction-induced demand side load management in residential buildings with user budget constraint[J]. Applied Energy,2017,187:352-366.

[52] Yongli Wang, Yudong Wang, Yujing Huang, et al. Planning and operation method of the regional integrated energy system considering economy and environment[J]. Energy,2019,171:731-750.

[53] Liu Xiaofeng, Gao Bingtuan, Wu Cheng, et al. Demand-Side Management With Household Plug-In Electric Vehicles: A Bayesian Game-Theoretic Approach[J]. IEEE Systems Journal,2018,12(3):2894-2904.

[54] Cunningham L. B., Baldick R., Baughman M. L. An Empirical Study of Applied Game Theory: Transmission Constrained Cournot Behavior[J]. IEEE Power Engineering Review,2002,22(1):166-172.

[55] Otero Novas I., Meseguer C., Batlle C., et al. A simulation model for a competitive generation market[J]. IEEE Transactions on Power Systems,2000,15(1):250-256.

[56] Chattopadhyay, Deb. Multicommodity spatial Cournot model for generator bidding analysis[J]. IEEE Transactions on power systems,2004,19(1):267-275.

[57] Hobbs, B. E. Linear complementarity models of Nash-Cournot competition in bilateral and POOLCO power markets[J]. IEEE Transactions on power systems ,2001,16(2):194-202.

[58] Tushar, Wayes, et al. Three-party energy management with distributed energy resources in smart grid[J]. IEEE Transactions on Industrial Electronics,2014,62 (4):2487-2498.

[59] Tushar, Wayes, et al. Prioritizing consumers in smart grid: A game theoretic approach[J]. IEEE Transactions on Smart Grid,2014, 5(3):1429-1438.

[60] Yu, Mengmeng, and Seung Ho Hong. Supply–demand balancing for power management in smart grid: A Stackelberg game approach[J]. Applied energy,2016,164:702-710.

[61] Lee, Joohyung, et al. Distributed energy trading in microgrids: A game-theoretic model and its equilibrium analysis[J]. IEEE Transactions on Industrial Electronics ,2015,62(6):3524-3533.

[62] Maharjan, Sabita, et al. Demand response management in the smart grid in a large population regime[J]. IEEE Transactions on Smart Grid,2015,7(1):189-199.

[63] Maharjan, Sabita, et al. Dependable demand response management in the smart grid: A Stackelberg game approach[J]. IEEE Transactions on Smart Grid,2013,4(1):120-132.

[64] Sheikhi, Aras, et al. Integrated demand side management game in smart energy hubs[J]. IEEE Transactions on Smart Grid,2015,6(2):675-683.

[65] Su, Wencong, and Alex Q. Huang. A game theoretic framework for a next-generation retail electricity market with high penetration of distributed residential electricity suppliers[J].Applied Energy,2014, 119:341-350.

[66] Solano J.C.,Caamaño-Martín E.,Olivieri L.,Almeida-Galárraga D.. HVAC systems and thermal comfort in buildings climate control: An experimental case study[J]. Energy Reports,2021,7(S3):269-277.

[67] 王海洋,李珂,张承慧,马昕.基于主从博弈的社区综合能源系统分布式协同优化运行策略[J].中国电机工程学报,2020,40(17):5435-5445.

[68] Mathias Berger, David Radu, Ghislain Detienne, et al. Remote Renewable Hubs for Carbon-Neutral Synthetic Fuel Production[J]. Frontiers in Energy Research, 2021, 2102:11375.

[69] The Engineering ToolBox. Met - Metabolic Rate[EB/OL].2004.[2022]. https://www.engineeringtoolbox.com/met-metabolic-rate-d_733.html.